People's Democratic Republic of Algeria
Ministry of Higher Education and Scientific Research

University M'Hamed BOUGARA – Boumerdès

Institute of Electrical and Electronic Engineering
Department of Power and Control

Project Report Presented in Partial Fulfilment of

the Requirements of the Degree of

'Master'

In Power Engineering

Title:

Design and Control of PEC9 Based Multifunctional Solar Active Filter

Presented By:

- **ABDELKEBIR Raham**
- **BELLOUZ Khaoula**

Supervisor:

-Pr. KHALDOUNE. Aissa

Registration Number:…/2025

DEDICATION

In the Name of Allah — All praise is to Him who grants success and knowledge. Peace and blessings be upon the Prophet.

To the light of my life, my beloved mother Chelfi Fadila — your love and prayers were the foundation of every success I've achieved. May Allah bless you in this life and the next. And to my dear father, Maachou — your strength and sacrifices guided me throughout. Thank you for your belief in me and your unwavering support.

To my sister Ahlem — your presence brought me comfort and support. Thank you for always being by my side. And to my little sister Assil — the joy of our home and a part of my soul. Your smile brightens my life, and your innocence brings peace to my heart. I hope to always be a role model you can look up to.

To my brother Akram — Thank you for your strength, care, and unwavering belief in me. And to my uncle Miloud — Your encouragement has always meant so much to me. I'm deeply grateful for your constant support.

To my respected professor,Khaldoune Aissa — Thank you for your guidance, your valuable time, and your sincere dedication. May Allah reward you for your efforts and wisdom.

To my self — Thank you for not giving up, even when things felt overwhelming. Thank you for the long nights, the silent tears, the patience, and the persistence. You turned challenges into growth and dreams into reality. Be proud — you've earned it.

And finally, to my friends and all who supported me — thank you for being part of the journey. This work is for you.

Khaoula.B

To my beloved father, Naoui, and my dearest mother, Zaoouche Khaira — you have been the light that guided my path and the lantern of my hopes. Thank you for every moment of support and encouragement. I dedicate this achievement to you; it is the fruit of your efforts and sacrifices.

To the souls of my grandparents — may Allah have mercy on them — I dedicate this thesis in loving memory of you both.

To my pillars in life, my companions throughout my academic journey — my brothers Boumediane and Zineddine — thank you for being my source of strength, and my beloved ones Slimane and salah.

To my beloved sisters: Hiyam, Fatima, and Loubna — thank you for your warmth and love.

To my dear sister-in-law, Leila Semane — the sister I never had by blood — thank you for every moment of support and care.

To my uncles and aunts, thank you for every heartfelt prayer you offered for me.

To the little ones who bring joy to my life: Abdelouahab, Ziad, Mohammed, Rahaf, chada Latin, and my sweet heart Meriem Assil.

To my dear friends Ratiba and Rima — thank you for standing by me through it all.

To the one who was a divine blessing in my life, the true embodiment of friendship — Soukehal Amina Hala — thank you for your unwavering support throughout this journey.

I dedicate this work to myself, for every moment I faced challenges and kept going, and to my thesis partner khaoula, who stood beside me every step of the way.

To my esteemed professor Khaldoune Aissa, Thank you for your knowledge, guidance, and unwavering belief in me. You have been a source of inspiration and motivation throughout this academic journey. I extend to you my deepest respect and gratitude.

And finally, to those who supported me silently, and to all my friends at INELEC — thank you for your presence and your encouragement.

Raham A.

Acknowledgements

Alhamdulillah, all praises to Allah for the strengths and His blessing in completing this thesis.

We would like to express our gratitude to our supervisor **Pr. KHELDOUN Aissa**, who guided us throughout this project and made this work possible. His guidance and advice carried us through all the stages of writing our project.

Special thanks to Dr. **KHETTAB Soufian** for his helpful tips and valuable remarks.

ABSTRACT

This work presents the control design of multifunctional solar active power filter based grid connected PV system, whose architecture basically consisted of utility grid, non linear load and Packed E-Cell inverter with PV (PV-PEC) generator as renewable source, connected in parallel through the point of common coupling.

The system designed to operate as an active power filter, to filter the harmonics caused by the non linear load. Based on the modified instantaneous power (PQ) theory the PV-PEC active power filter extracts the fundamental harmonics components from the load current to generate a reference current. This reference current is then tracked using a Finite Set Model Predictive Control (FS-MPC) strategy, enabling the system to inject compensating currents into the grid while simultaneously extracting maximum power from the PV source.

Moreover, we have investigated a new inverter topology that is the PEC nine level inverter (PEC9). It stands out as a superior choice compared to conventional topologies in terms of power quality improvement, total harmonic distortion reduction reduced switch count, and multilevel voltage production with a propre control.

Keywords—Solar active power filter (SAPF), Photovoltaic (PV), Maximum power point tracking (MPPT), modified instantaneous power theory (p-q), Total harmonic distortion (THD), Packed E-cell 9 levels inverter (PEC9), Perturb and observe (P&O), Finite Set Model predictive control (FS-MPC).

Table of Contents

List of Figures

List of Tables

LIST OF ABBREVIATIONS

AC Alternating Current

APF Active Power Filters

BPF Band-Pass Filter

DC Direct Current

FS MPC Finite Set Model Predictive Control

HAPF Hybrid Active Power Filters

HB Hysteresis Band

HCC Hysteresis Current Control

HPF Hybrid Pass Filter

IEEE Institute of Electrical and Electronic Engineers

IGBT Insulated Gate Bipolar Transistor

LPF Low-Pass Filter

MOSFET Metal Oxide Semiconductor Field Effect Transistor

MPC Model Predictive Control

MPPT Maximum Power Point Tracking

P&O Perturbation and Observation

PCC Point of Common Coupling

PEC9 Packed E Cell Inverter

PF Power Filters

PLL Phase Locked Loop

PSO Particle Swarm Optimization

PQ Power Quality

PUC Packed U Cell Inverter

PV Photovoltaic

PWM Pulse Width Modulation

SAF Solar Active Filters

SAPF Shunt Active Power Filter

STC Standard Test Condition

THD Total Harmonic Distortion

VSI Voltage Source Inverter

GENERAL INTRODUCTION

In recent decades, the increasing demande for electricity and the urgent need to reduce environmental pollution produced by conventional energy sources, have been accelerated the integration of renewable energy sources, particularly photovoltaic (PV) system into electrical grids [1]. They gain a significant role in electrical power generation systems in order to minimize the drawbacks caused by the use of fossil fuels.

However, maintaining a good power quality level, voltage regulation and low harmonic distortion in modern electric grids remains the greatest challenge in front of the non-stop harmonic pollution generated by the nonlinear and unbalanced loads [2]. multifunctional power electronic converters have emerged as effective solutions to enhance the performance and reliability of distributed generation system [3].

Conventional inverters used in PV systems mainly focus on energy injection without addressing power quality issues. Thus, to achieve a high power quality in the grid connected PV systems, a novel topology of Multifunctional Packed E-Cell (PEC) inverter is proposed to overcome the extended PUC drawbacks in which one E-cell substitutes two U-cells [4].

A Nine level packed E-cell (PEC9) inverter operating as a multifunctional solar active power filter based grid connected PV system is proposed in this report. The PV system designed with a PV array and DC-DC boost converter to inject power to the utility grid without any need of energy storage device. The DC-DC converter ensure the extraction of the maximum power from the PV array using Perturbation and Observation control technique.

PEC9 converter topology stands out as a superior choice compared to packed U-cell converters structure and conventional inverters due to its higher power conversion efficiency, small filter, low voltage stress across semiconductor switches and less total harmonic distortion in the output voltage and current [5].

the main role of PEC9 - SAPF is to inject proper compensation current at the point of common coupling (pcc) in a way that the harmonics produced by the non linear load are suppressed and the grid current is a pure sine wave in phase with the grid voltage [2].

A finite set MPC technique is developed to enable the inverter to operate in active power filtering and power injection mode. The main objective of this thesis is to design a proper control strategy for multifunctional PEC9 inverter to perform solar power injection by PV array with low THD and eliminate harmonic currents content at the PCC.

This report is structured as follows:

- Chapter I: provides an overview of modern power generation, highlighting the necessity of renewable energy sources integration. In addition to the concept of power quality and issues, harmonics as the main concept of this project with a brief description of mitigation techniques.

- Chapter II: explains the needed background to understand the system modeling, providing detailed descriptions of PV systems and active filters.

- Chapter III: presents a detailed description of the system configuration, the mathematical modeling of its components, and the control strategies implemented to achieve the desired objectives.

- Chapter IV: presents simulation results and performance evaluation, of the proposed PEC9-based solar active filter.

Finally , a general conclusion that summarizes the present project ,and its overcomes as well as the future research directions.

CHAPTER 1

POWER SYSTEM AND CHALLENGES

1.1 Introduction

Modern power systems are complex networks designed to generate, transmit, and distribute electrical energy. Although power quality (PQ) problems in power utility distribution networks are not modern, their consequences have become more relevant in recent years. They may also be explained as the degree to which the supplied power is compatible with the smooth operation of the electrical equipment [6].

Power electronics equipment which involves adjustable speed motor drives, electronic power supplies, battery chargers, and DC motor drives appears to be the main causes of harmonic distortion in a distribution system, causing an increase in PQ-related issues. Harmonics have a variety of undesirable consequences in the distribution network. In grid-connected systems, several current and voltage harmonics affect the system performance.

Active power filters (APFs) and passive filters (PFs) are efficient solutions utilized to address PQ issues .Passive filters utilize a more simple, traditional approach to resolving power quality issues, but can impose extra costs with size and inflexibility in high power environments .Comparatively, APFs provide flexible dynamic compensation in power quality issues, making it the more preferred, effective, and efficient on the modern electrical networks [7].

1.2 Electrical power generation

The recent global increase in demand for electricity has been associated with another demand - rising living standards, industrial expansion and economic development. As energy consumption continues to increase, planning in the power sector is required to produce enough electricity sustainably. The environmental and social consequences of traditional fossil-fuel based power plants - air pollution, greenhouse gas emissions, resource depletion meant that governments and researchers alike, were interested in cleaner ways of producing electricity. Within this frame of reference, clean, renewable energy sources offer alternatives to meet energy demand while encouraging environmental sustainability and economic diversification [1].

1.3 Power Quality

Power quality (PQ) has emerged as a critical concern for electricity consumers across all usage levels it is defined as a measure of how well a power system supports smooth operation of its loads [6]. The broadening use of power electronics-based devices, including switch-mode power supplies (SMPS), dimmers, current regulators, frequency converters, energy-saving lamps, and arc welding machines with non linear characteristics, adversely affects the quality of consumers electric power supply due to their inherent non-linear loads. Harmonics are produced when these devices distort the power system waveform by improperly introducing frequency components into it, which can lead to overheating, equipment malfunction, and increased losses.

Furthermore, the growing integration of renewable energy sources into power generation has added complexity to power distribution networks. Although renewables are essential for sustainable energy, their intermittent nature and associated power electronics can exacerbate PQ issues, making the electrical system more susceptible to disturbances. Consequently, both utilities and end-users are increasingly concerned about maintaining high power quality. Efforts to mitigate these challenges include the implementation of harmonic filters, voltage regulators, and advanced monitoring systems to ensure the reliability and efficiency of the power supply.

1.4 Grid Connected PV System

Around 99 % of installed PV capacity worldwide is made up of grid-connected systems as opposed to standalone, battery-powered systems. PV systems connected to the grid without batteries are less expensive and require less maintenance. The resultant power is uploaded to the grid for consumption, distribution, and direct transmission. As a result, other sources of grid electricity are less burdened. A specific amount of power is generated by the grid, load, and PV array that make up the network. Control features like Maximum Power Point Tracking (MPPT) are built into a DC/DC converter, which work as a power optimizer. Through a DC/AC inverter, the PV system is connected to the grid [8] as illustrated in figure 1.1.

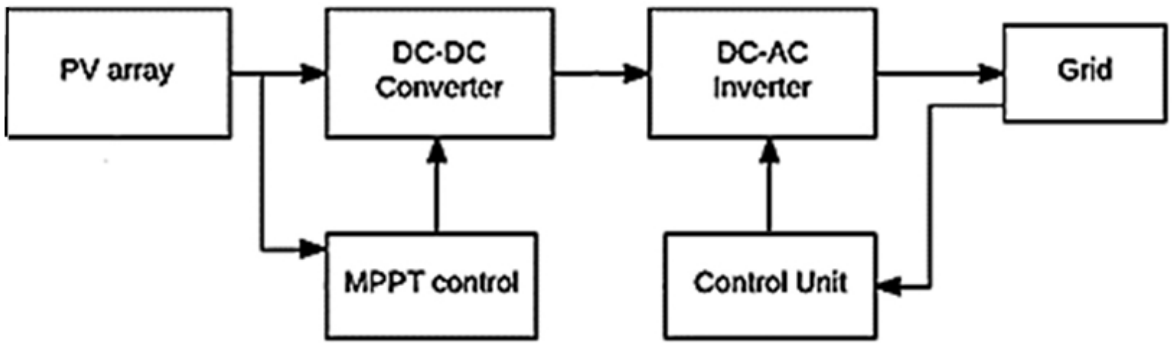

Figure 1.1: Grid connected PV system

1.5 Types of Power Quality Issues

Power quality issues are defined as any power problem manifested in voltage, current, or frequency deviations that results in failure or miss-operation of customer equipment [9]. The following are the most common types of Power Quality issues:

- Voltage sag (or dip):

  A decrease of the normal voltage level between 10% and 90% of the nominal rms voltage at the power frequency, for durations of 0,5 cycle to 1 minute [10] (see figure 1.2).

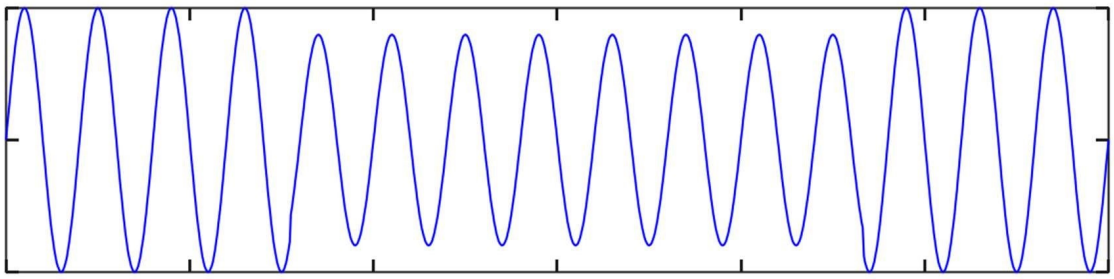

Figure 1.2: Voltage waveform during voltage sag

- Interruptions: Which refer to the power

  Short interruptions: Total interruption of electrical supply for duration from few milliseconds to two seconds [10].

  Long interruptions: Total interruption of electrical supply for duration greater than to 2 seconds and less than two minutes [10].

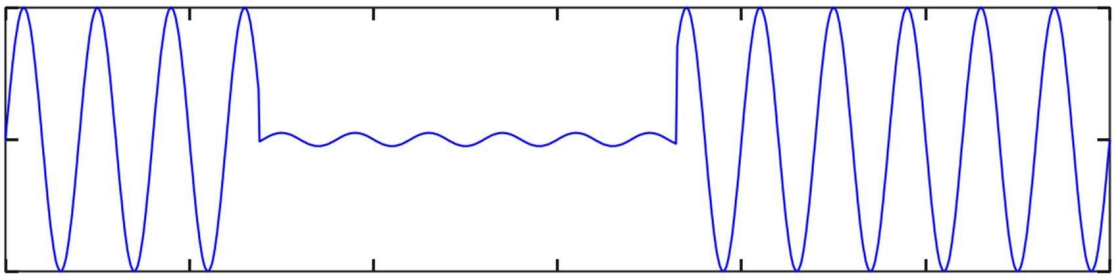

Figure 1.3: Voltage waveform during an interruption

- Voltage spike: Very fast variation of the voltage value for durations from a several microseconds to few milliseconds. These variations may reach thousands of volts, even in low voltage [10] see figure 1.4.

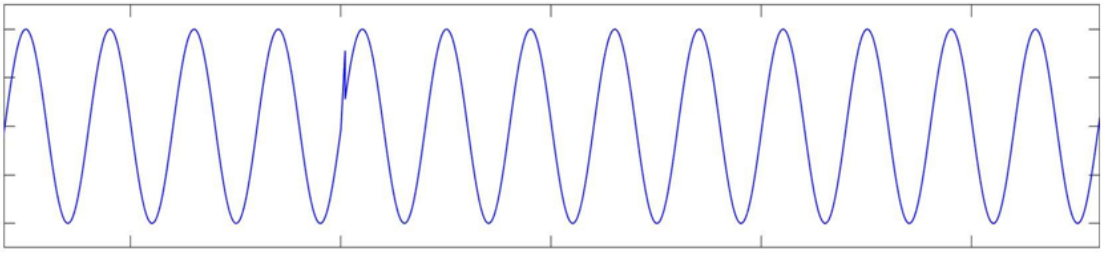

Figure 1.4: Voltage waveform during spike

- Voltage swell :Momentary increase of the voltage , at the power frequency, outside the normal tolerances , with duration of more than one cycle and typically less than a few seconds [10] as shown in figure 1.5.

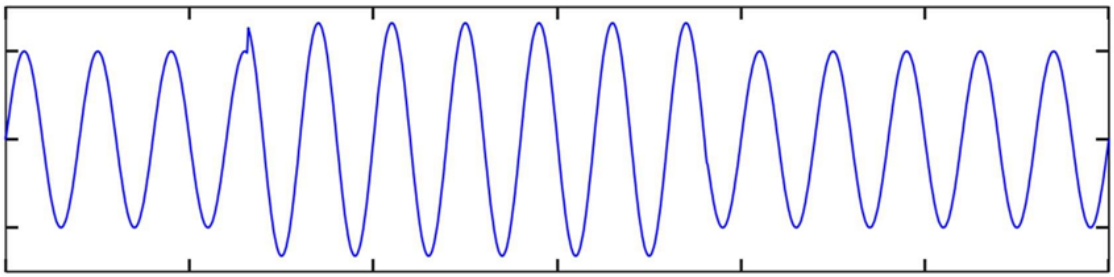

Figure 1.5: Voltage waveform during swell

- Harmonic distortion :Voltage or current waveforms assume non-sinusoidal shape. The waveform corresponds to the sum of different sine waves with different magnitude and phase, having frequencies that are multiples of power-system frequency [10].figure 1.6 illustrates an example of harmonic distortion.

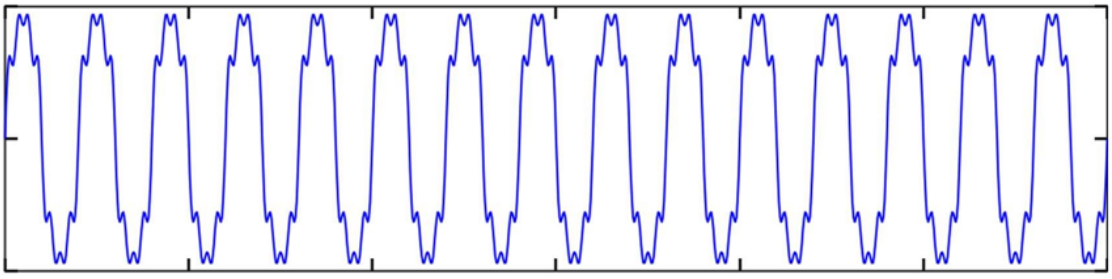

Figure 1.6: Voltage waveform during harmonics

- Noise: An unwanted electrical signal of high frequency from other equipment [10] that affects with current or voltage waveforms .figure 1.7 shows an example.

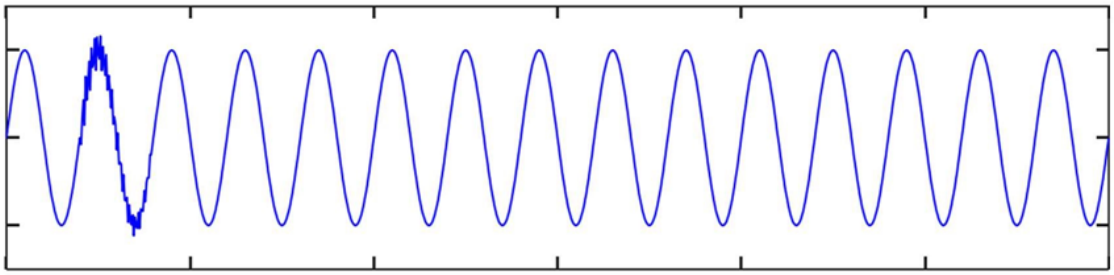

Figure 1.7: Voltage waveform during noise

- Voltage fluctuation : Oscillation of voltage value, amplitude modulated by signal with frequency of 0 to 30Hz [10] which may result in the voltage that look like the one shoen in figure 1.8.

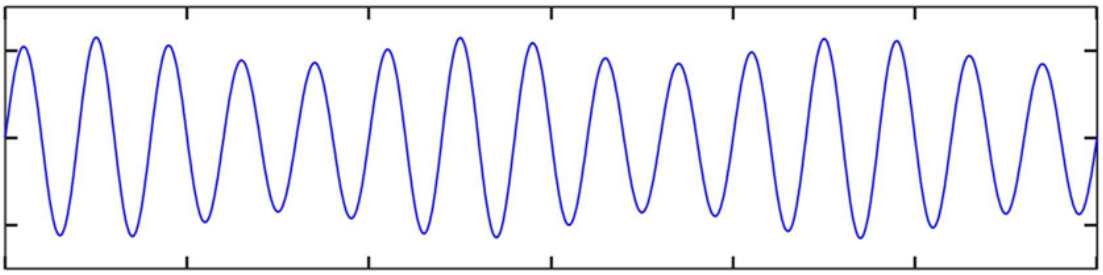

Figure 1.8: Voltage waveform during fluctuation.

- Voltage Unbalance: A voltage variation in a three-phase system in which the three voltage magnitudes or the phase-angle differences between them are not equal [10]. figure 1.9 illustrate an unbelanced three phase voltage.

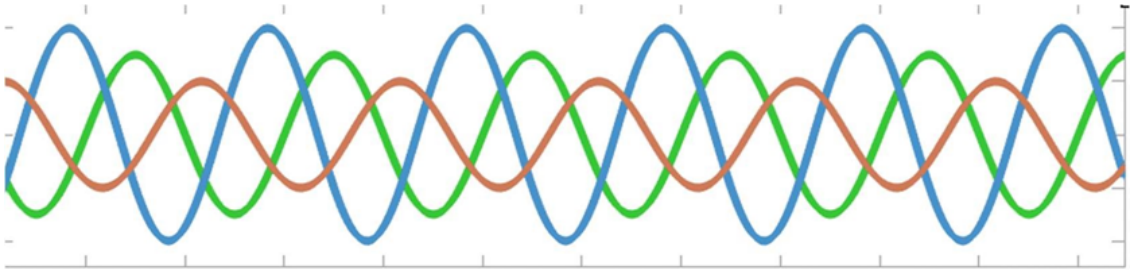

Figure 1.9: Voltage waveform during voltage unbalance .

1.6 Harmonics in Power Systems

Harmonics are distortions to voltage and current sign waves. If equipment in an industrial facility operates by altering sign wave behavior between AC and DC, it will cause harmonic distortion.

1.6.1 Voltage and Current Harmonics

The effects of voltage and current harmonics are distinct, yet they are also connected. Harmonic currents appear to be injected into the power system by nonlinear loads at the consumer end. As a result, they are sometimes considered as harmonic current sources. In addition to that, the harmonic voltages are the consequence of harmonic current times the control system's linear impedances. The voltage drops across the system resistances caused by the harmonic current passing through it results in voltage harmonics. Thus, the later are a function of current harmonics and the power system's linear impedances. Figure 1.10 shows a voltage waveform of peak value equal to the secondary distribution level i.e. 220 V. Likewise, it also depicts the harmonics mechanisms with amplitudes of (1/3) to (1/5) and (1/5) to (1/7) of 220V and having the frequencies three, five and seven times the essential frequency correspondingly. Assuming the voltage harmonics are due to the passage of harmonic current through a system resistance [11]. Sinusoidal 50 Hz waveform with 3rd, 5th and 7th Harmonics.

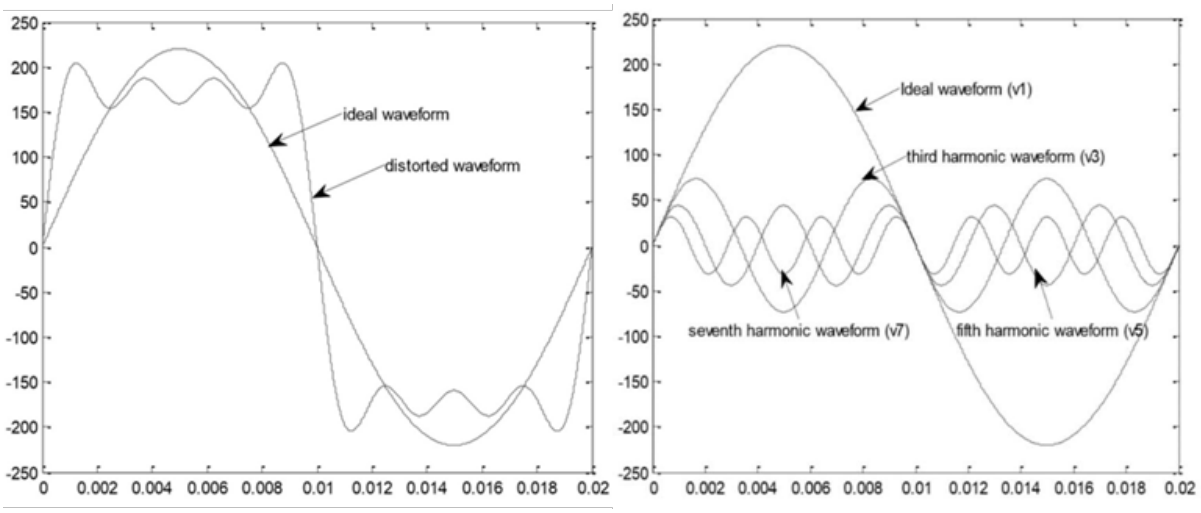

Figure 1.10: Sinusoidal 50 Hz waveform with 3rd, 5th and 7th Harmonics.

1.6.2 Harmonic Sources

Harmonics in electrical power systems arise from various components. Transformers produce harmonic distortions, especially under non-ideal conditions or in saturation. Large electrical machines, such as motors and generators, and those combined with renewables have been connected at many levels of voltage, and now are assumed to inject harmonic currents. High Voltage Direct Current (HVDC) transmission systems and their converter stations are well known to be major contributors to harmonics due to their excessive use of power electronic switching devices with non-sinusoidal waveforms [12].

1.6.3 Impact of Harmonics on Power Systems

Harmonics can be very harmful to the power system as well as any attached equipment in the power system. The effects of voltage and current harmonics in the power system can be summarized as follows [11]:

- The potential for amplification of harmonic levels caused by series and parallel resonance.
- Overheating in the phase and neutral conductors.
- Degradation of generator efficiency caused by harmonics.
- Eddy current and hysteresis losses in transformers.

- Overheating of the system components e.g. generators, motors, transformers, etc.
- Additional current flow through power capacitors.
- Decrease in operating life of incandescent lamps.
- Skin effect and proximity effects increased.
- Interference problem with telecommunication.
- Issues with the relay protection system.

1.6.4 Mitigation Strategies for Harmonics

As mentioned before, harmonic distortion has become a growing concern in modern electrical power systems due to the widespread use of nonlinear loads and power electronic devices. These distortions can lead to significant issues , to preserve system stability and ensure compliance with international power quality standards the following sections present an overview of the most common and effective harmonic mitigation strategies [13].

1.6.4.1 Conventional Harmonic Mitigation Methods

The simplest conventional solution to mitigate the harmonic distortion is passive filtering. Despite their simplicity, the dynamics of the power distribution systems are not always adequately responded by passive elements. Through the years, these passive filters have been developed for a high level of sophistication [14].

Conventional passive filters consist of inductance, capacitance, and resistance elements configured and tuned to control harmonics to specific frequencies to provide low-impedance paths [14].

They can be classified into several types according to the harmonic frequencies they are designed to mitigate :

- **Series Line Reactors**

  Line Reactors are the simplest and lowest cost means of attenuating harmonics. They connect in series with an individual non-linear load to limit the flow of harmonic currents by increasing the source impedance ,as well as absorb voltage transients [14].

- **Tuned Harmonic Filters**

  They're the most common and most affordable type of passive filter. They are typically designed as LC circuits tuned to a specific harmonic order .The LC circuits are connected in parallel with the non linear load to provide a low-impedance path at the tuned frequency, and divert harmonic currents away from their normal flow path through the filter, and reduce voltage and current distortion [14].

  Tuned filters are widely used in industrial environments where harmonic sources are predictable and relatively constant. Despite their effectiveness at targeted frequencies, they may resonate with the power system and are sensitive to system impedance variations, which can limit their performance under dynamic load conditions.

- **High Pulse Converters**

  High-pulse converters provide an effective means of minimizing harmonic distortion at source through the use of rectifier bridges and phase-shifting transformers. These converters can operate using rectifier bridges through 12-pulse, 18-pulse, or even 24-pulse arrangements and phase-shift the AC input to each rectifier module so that the harmonic currents produced by one rectifier cancel out the harmonic currents of the other rectifiers. This cancellation of harmonic currents results in significant minimization of the low-order harmonics (5th, 7th, 11th, and 13th) of the line current, which provides better power quality [14]. They are commonly used in medium and high-power industrial drives.

1.6.4.2 Advanced Harmonic Mitigation Methods

Traditional harmonic mitigation techniques have become insufficient in many applications. This has led to the development of advanced harmonic mitigation methods,which offer dynamic, adaptive, and more precise control over power quality.These techniques typically rely on power electronic converters, digital signal processing, and real-time control algorithms to actively detect and compensate harmonic components [7].these methods are known as active filter.

Active filters generally monitor load currents, eliminate fundamental frequency currents, assess the frequency and amplitude of the residuals, and subsequently inject the

corresponding inverse current or voltage to cancel the specific harmonics [14]. Depending on the application, APFs can be implemented in different configurations, primarily as shunt or series types, each with distinct roles in harmonic mitigation and voltage compensation.

- Shunt Active Power Filters (SAPFs) or parallel active power filters are the most commonly used type of active filters. They are are connected in parallel with the nonlinear load.as shown in the figure 1.12 the SAPF generates equal but opposite harmonic currents through a voltage source inverter (VSI). This action ensures that the source current remains nearly sinusoidal and in phase with the supply voltage, thus improving power factor and reducing total harmonic distortion (THD) [15].

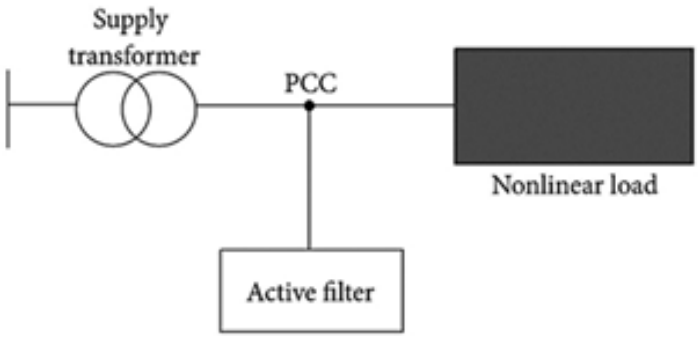

Figure 1.11: Shunt active power filter

- Series Active Power Filters are connected in series with the power supply line using a matching transformer as shown in the figure below. They focus on mitigating voltage harmonics, voltage sags, swells, and unbalances caused by nonlinear or unbalanced loads.

  They function by injecting a controlled voltage in series with the supply to ensure that the voltage across the load remains sinusoidal and within acceptable limits [7].

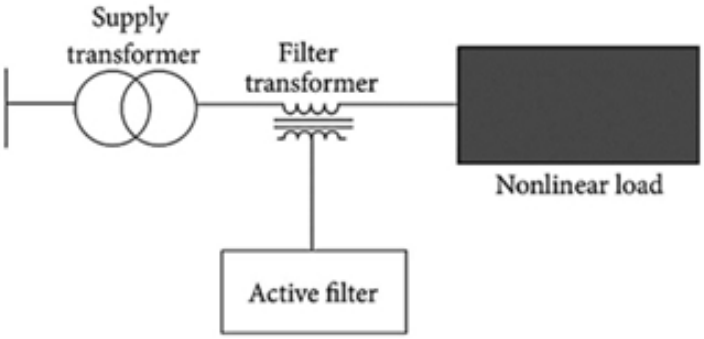

Figure 1.12: Series active power filter

1.6.4.3 Hybrid Harmonic Mitigation

Hybrid harmonic mitigation techniques combine the advantages of both passive and active filtering methods to provide a more efficient and cost-effective solution for power quality improvement. Passive filters handle lower-order harmonics and supply reactive power, while active power filters compensate for higher-order harmonics and dynamically changing loads by using the switching-mode power converter different configuration of hybrid active filter are available in litterature as shown in figure 1.13 [15].

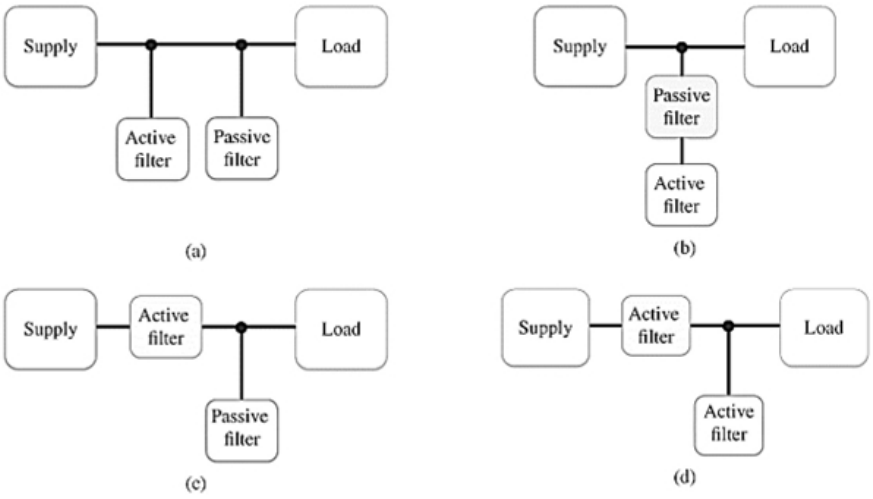

Figure 1.13: Hybrid connections of active and passive filters

1.7 Conclusion

This chapter has discussed the diverse causes and impacts of harmonics in power systems, highlighting the increasing necessity of effective mitigation techniques. Poor power quality

manifested through voltage sags, swells, harmonics, flicker, and interruptions—can lead to equipment failure, increased losses, and less efficient systems. Both conventional and advanced methods offer valuable tools for maintaining stable and clean power supply. The next chapter will cover the system modeling .

CHAPTER 2

System Modeling

2.1 Introduction

The multifunctional solar active power filter (SAPF) system that is proposed combines a photovoltaic (PV) energy source with an active power filtering action to extract the maximum power from the PV array while compensating for current harmonics caused by nonlinear loads, simultaneously. The overall system architecture includes a photovoltaic generator, a DC-DC boost converter, DC-link capacitor, a multi-level DC-AC inverter (PEC9), nonlinear load in the form of a full-bridge rectifier with passive components, and connection to an AC grid. The boost converter is controlled by the Perturb and Observe (P and O) algorithm to perform maximum power point tracking (MPPT) in order to extract the maximum amount of energy from the PV source. The PV array operates as a DC power supply feeding both the grid and the inverter based SAPF in parallel, allowing for harmonic mitigation and power injection into the grid.

2.2 Structure of Photovoltaic System

The PV system is layered and starts with the photovoltaic (PV) cell - this is a semiconductor device that allows the conversion of sunlight energy directly into DC electricity. Many PV cells comprise a PV module which is the principal functional unit designed for outdoor use. Many PV modules are also arranged in series and parallel formation as a PV array. The PV array is the unit of current generation for the PV system and the output is intended to satisfy power needs. Actual output power from a PV array will depend on both sunlight and temperature. DC-DC converters with MPPT (Maximum Power Point Tracking) functionality enhance the energy worth extracting from the PV array. If the output from the PV array is being utilized as DC electrical power, typically for any storage or direct use, the user can utilize the power for whatever the end-user intends. If the DC electrical power is destined for the grid, the option will require a converter, or inverter, to produce an AC electrical output. The PV system structure is modular, allowing applications for anything from homes to utility scale [16].

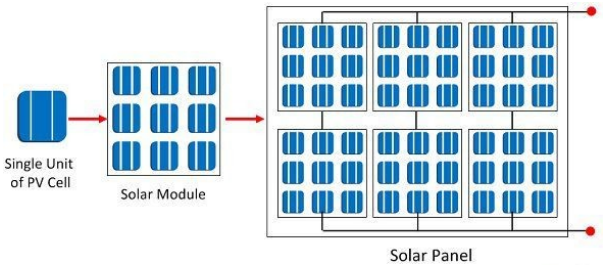

Figure 2.1: photovoltaic cell, module and array

2.3 Solar Photovoltaic Cell

Solar cell is a basic unit, which constructs the PV system. It consists of semiconducting material such as germanium and silicon. Silicon is used normally because its advantage over germanium [17] . When light strikes the solid surface of a semiconductor material, holes and electrons are created when light breaks the covalent bond in the semiconductor material's atom. Consequently, the terminals' polarity becomes positive or negative. The configuration of the PV cell is in a square or circular shape.

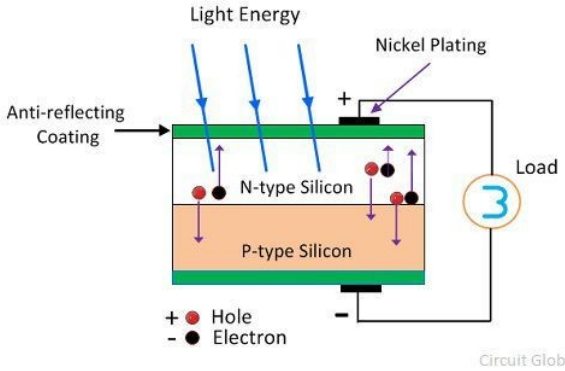

Figure 2.2: Basic operation of a photovoltaic cell diagram

To model the PV cell, a double and single based equivalent circuit are widely used as shown in Figure 2.3. The shunt and series resistances Rsh and Rp are the internal resistances of the PV Cell.

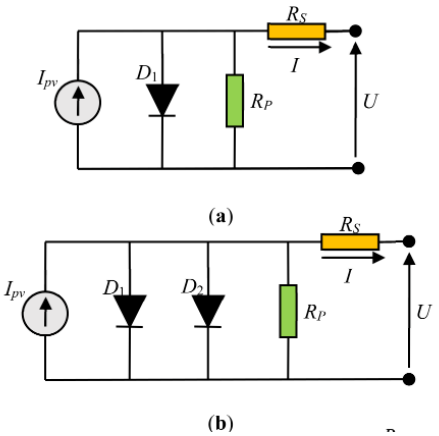

Figure 2.3: a) single and b) Double diode models equivalent circuits

The current I_{PV} generated by the PV cell, can be computed by:

For single diode model:

$$I_{PV} = I_{Ph} - I_D - I_{Sh} \tag{2.1}$$

For double diode model:

$$I_{PV} = I_{Ph} - I_{D1} - I_{D2} - I_{Sh} \tag{2.2}$$

Where I_D can be computed by:

$$I_D = I_S \left(e^{\left(\frac{V_{PV}+I_{PV}R_S}{V_T N_S}\right)} - 1 \right) \tag{2.3}$$

And:

$$I_{Ph} = I_{Ph} \times \frac{G}{G_{STC}} \tag{2.4}$$

$$V_T = \frac{AKT}{q} \tag{2.5}$$

V_{PV}: Output voltage across the PV cell.

I_{PV}: Output current across the PV cell.

A: Diode ideality constant.

I_{Ph}: Total photon current of the PV module.

K: Boltzmann's constant.

R_{sh}: Shunt resistor.

q: The charge constant.

R_S: Series resistor.

I_S: Diode saturation current.

G: Solar irradiation .

G_{STC}: Standard test condition irrediance 1000 w/m2.

$I_{Ph,STC}$:Photovoltaic or light generated current at STC.

N_S:Numberof pv cell in series .

The current versus voltage (I-V) and power versus voltage (P-V) characteristics measured for a single PV cell khow and are displayed in figure 2.4. Understanding the electrical I-V characteristics of a solar cell or panel is essential for identifying the output performance of the device and solar efficiency. [18] .

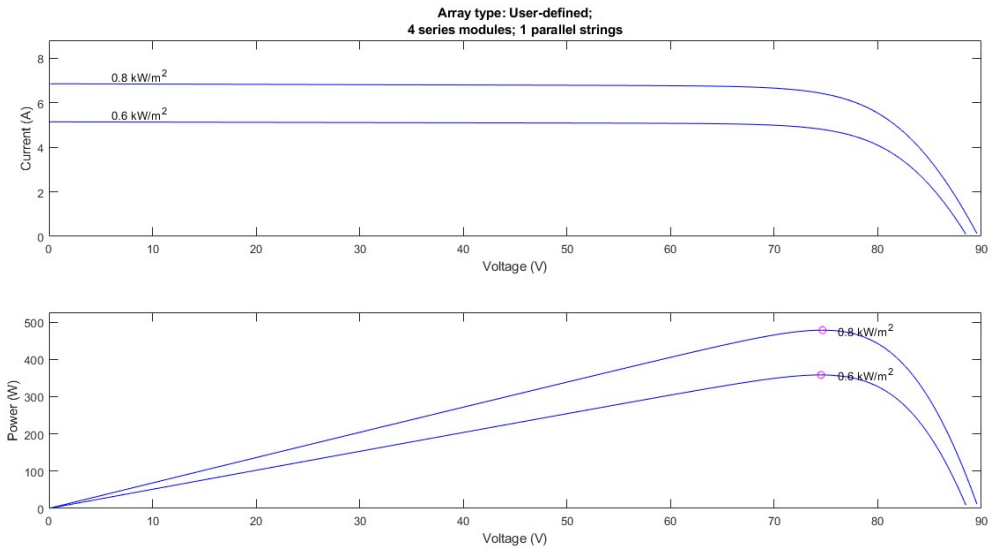

Figure 2.4: Current vs voltage (I-V) characteristics of PV cell and power vs voltage (P-V) characteristics of PV cell.

2.4 PV module

A single photovoltaic (PV) cell produces typically very little power, usually between 0.1-2 watts, which is not enough power for most viable applications. In order to get more power, multiple PV cells are interconnected with each other. PV cells are typically interconnected in series, forming a solar module, so that the total output voltage and power add together. Since a solar cell's voltage is about 0.5 volts, then 36- solar cells are interconnected in series to create a solar module outputting about 18 volts (0.5 V $\times$ 36). The watt power rating of one PV module can vary widely anywhere from 3 watts to

300 watts. Therefore, solar modules can be designed by including the right combination of cells that collectively provide the needed power output and satisfy commercial energy requirements. Typically these solar modules are called PV modules [19].

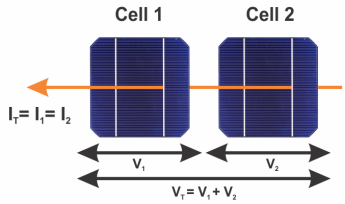

Figure 2.5: Series connected PV cells

2.5 PV array

A photovoltaic array is made up of a number of photovoltaic panels or modules that are electrically connected. Then can provide enough energy to operate applications that, when run off a single photovoltaic module, would not have enough energy. Because a single photovoltaic modules out is few watts, these are combined together, and can be connected in series to produce higher voltage, connected in parallel to increase current or a combination of both to provide the desired power output. This modular arrangement can provide flexibility when designing solar power systems with different voltage and current requirements and by using more overall surface area of solar energy produced based on the photovoltaic array's size [20]

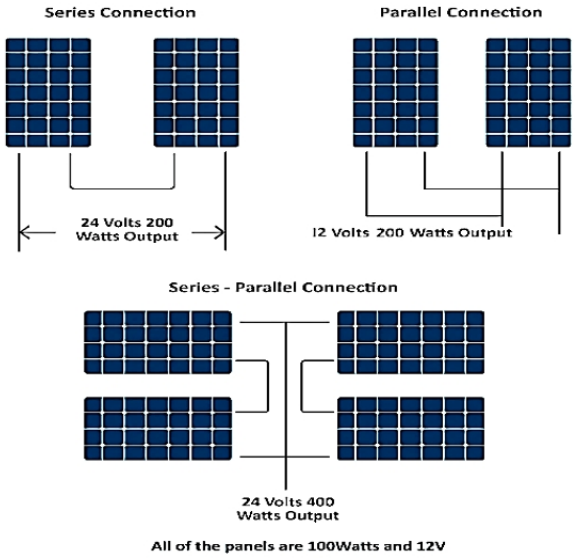

Figure 2.6: Connections of solar panels (modules)

2.6 Maximum power point of solar array

Under Standard Test Conditions (STC), the V–I characteristic curve of a solar cell has a distinct bending point, same commonly call the knee point. The solar cell provides the maximum electrical power (Pm) at that point. This is the optimal operating point of the solar cell where the power product is maximized.

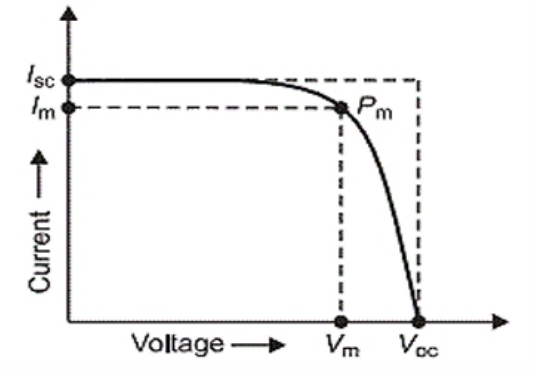

Figure 2.7: V-I characteristics of PV array

In the V-I characteristics of a solar cell, Im represents the current at maximum power point, while Vm represents the voltage at maximum power point.

2.7 PV Array Characteristic Curves

2.7.1 Current Versus Voltage and Power Versus Voltage Curve

The two key points on the current–voltage (I–V) curve for a PV module are the current at the maximum power point (Im) and the voltage at the maximum power point (Vm).

The short-circuit current (Isc) is the current flowing into a shorted PV module, or when the voltage at the two terminals of the module is zero. Thus, this is the current that describes the maximum current and gives rise to the Power versus Voltage (P–V) curve, which is also shown as the red line in Figure 2.8.

The open-circuit voltage (Voc) describes the terminal voltage when the terminals are open and the current is zero.

Connecting a load across the two terminals of a PV module results in a voltage and current between Isc to Voc and doesn't tell us anything about the output power of the

PV module except for the I–V curve itself, which is shown as the blue line in Figure 2.8. However, once we have the I–V curve of the PV module, we can calculate the output power of the PV module at different operating points.

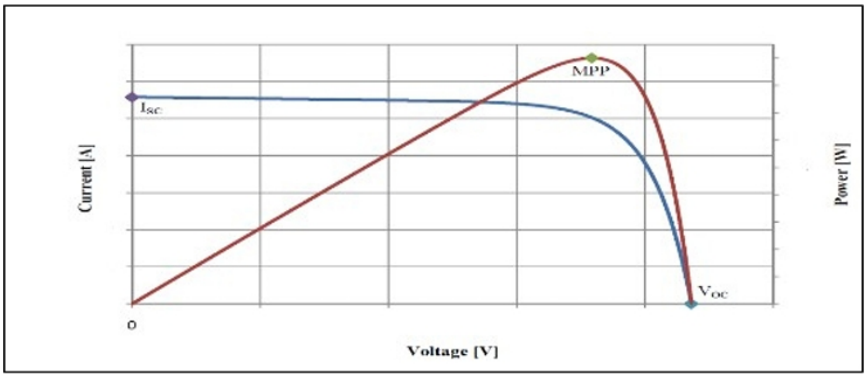

Figure 2.8: current and power versus Voltage curve

2.7.2 Effect of Solar Irradiation on Characteristic Curves

The I-V curve and P-V curve are affected by the solar irradiation. When the solar irradiation change the maximum power point of the solar module will change also [21], so the technique MPPT is used to trace the maximum power to have the maximum efficiency of the module. When more solar irradiation fall on the surface of the solar module the excitation energies of the electrons will increase means the electrons will have higher mobility level which can produce more power. In these cases, the short circuit current will increased as shown in the figure (2.9) and the open circuit voltage remains almost the same [22]. The atmospheric conditions affect the irradiation which is therefore varying in the month or a day, could also vary significantly due to fast changing conditions because of clouds. In other words, the solar module needs MPP technique to assure that the module gives maximum possible power always at any condition as well to have maximum efficiency of the module.

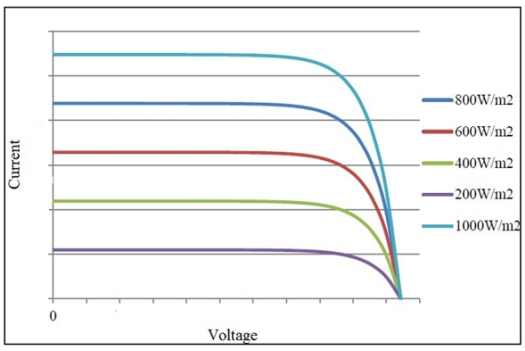

Figure 2.9: Effect of changing solar irradiation on I-V curve.

2.8 Maximum Power Point Tracking (MPPT)

Maximum power point tracking (MPPT) is a method that can optimize the power generation of a photovoltaic system under different environmental conditions. The MPP of the PV array is a unique point where maximum power is achieved, and this operating point corresponds to a unique PV voltage and current value the array has at that specific environment and load condition. The Perturb and Observe (P and O) is one of the most well-known MPPT algorithms, it functions by slowly varying the voltage or current of the PV array and noting the power produced. The MPPT controller will continue to adjust the voltage or current (by changing the duty cycle of the chopper) in the same direction as long as the power keeps increasing. When the power decreases, the controller will adjust the control signal in the opposite direction. This will continue until the also many times as required, to establish that the variation of the power with respect to the change of voltage or current is zero. This point is known as the MPP of the P/V characteristic. These actions are reduced to a flowchart for the P and O technique given in Fig3.11. The P and O algorithm, as can be seen from the flowchart, is simple, straight forward and therefore widely used [23]

2.9 Boost converter

A boost converter is a kind of DC/DC switch mode power supply that increases (boost) the input voltage from a direct current (DC) input, such as a photovoltaic (PV) array, to a constant, higher output voltage. The important components of a boost converter include an inductor, a semiconductor switch (typically a MOSFET), a diode, and a capacitor.

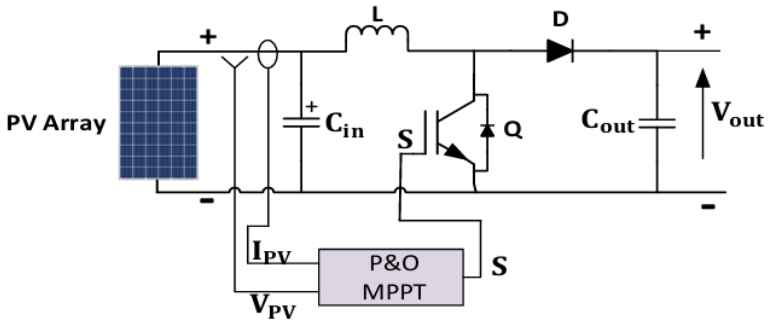

Figure 2.10: DC-DC boost converter with MPPT

A boost converter with MPPT control via the P and O method has been realized. The aim is to reach the MPP by changing the output voltage of the PV panel. A simplified diagram of a PV DC-DC boost converter with MPPT is shown in Figure 2.10. The output voltage of the converter (Vout) and the input voltage (VPV) is expressed in Equation (2.5)

$$V_{\text{out}} = \frac{V_{pv}}{1 - D} \tag{2.6}$$

Here, (D) represents the duty cycle of the MOSFET switch. The duty cycle is modified through a PWM signal, applied to the gate of the MOSFET. The boost converter will adjust the duty cycle of the MOSFET switch to maintain the output voltage based on the solar energy available.

2.10 DC-AC Inverter

An inverter is a very important part of a solar energy system. It is the interface of a solar renewable energy system to the grid at the distribution level. An inverter converts the DC voltage generated by a PV array into an AC voltage. The inverter produces an AC voltage that is equal to the grid supply voltage and at the same frequency. This is accomplished by using controlled switching devices like MOSFETs, the inverter turns the switches on and off continuously, and the grid interfacing inverter then takes on added responsibilities of shunt active power filter in our system.

2.10.1 Classical Two-Level Inverter

A two-level single-phase inverter is a basic power electronic device used for changing a DC input voltage into an AC output voltage. It does this by changing the output voltage to two discrete levels, with the two voltages typically being the two polarities of the DC supply (positive and negative). The inverter can be implemented in a half-bridge or full-bridge topology, and can be built with several semiconductor devices as shown in figure 2.11. The semiconductor switches in the inverter circuitry are arranged so that the switches operate in a complementary fashion, meaning that when one switch in a leg (called a "switching leg") is selected to be "ON," the other switch in the leg must be "OFF" to prevent short-circuiting the DC source. The basic output voltage waveform is a square wave and the inverter uses pulse width modulation (PWM) so that the inverter can create a single frequency controllable sinusoidal output voltage with controllable frequency and amplitude. The technical ease of design, versatility of applications, and effective performance in practice makes the two-level single-phase inverter very useful for a wide range of applications (for example: residential solar power systems, uninterruptible power supplies, small motor drives, etc) requiring a reliable and efficient DC-to-AC conversion [24]

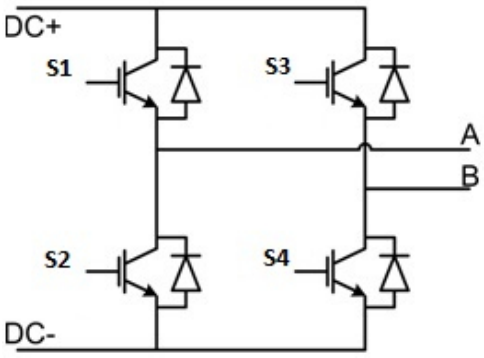

Figure 2.11: Two-level single-phase inverter

A two-level single-phase inverter uses four switches arranged in two legs, with complementary switching in each leg to prevent short circuits. The output voltage switches between +Vdc and -Vdc depending on which switches are ON, producing two active states for positive and negative voltages and two zero states with zero output voltage. This simple switching scheme enables safe and effective DC-to-AC conversion.

Table 2.1: Switching States of 2-Level Single-Phase Full-Bridge Inverter

No.	S1	S2	S3	S4	V_{out}
1	ON	OFF	OFF	ON	$+V_{dc}$
2	OFF	ON	ON	OFF	$-V_{dc}$
3	OFF	ON	OFF	ON	0 (ZVS)
4	ON	OFF	ON	OFF	0 (ZVS)

2.10.2 Packed E-Cell 9-level inverter (PEC9)

The single-phase topology of the PEC9 inverter is shown in Fig 2.12, which is designed based on a comptonization of half-bridge and the E-Cell . PEC9 consists of 6 active switches (S1,. . . .S6), one four-quadrant bidirectional switch (S7), one dc source Vdc and two capacitors C1 and C2. The structure of Figure 2.12.is connected to a utility by R-Last as the grid filter [25].

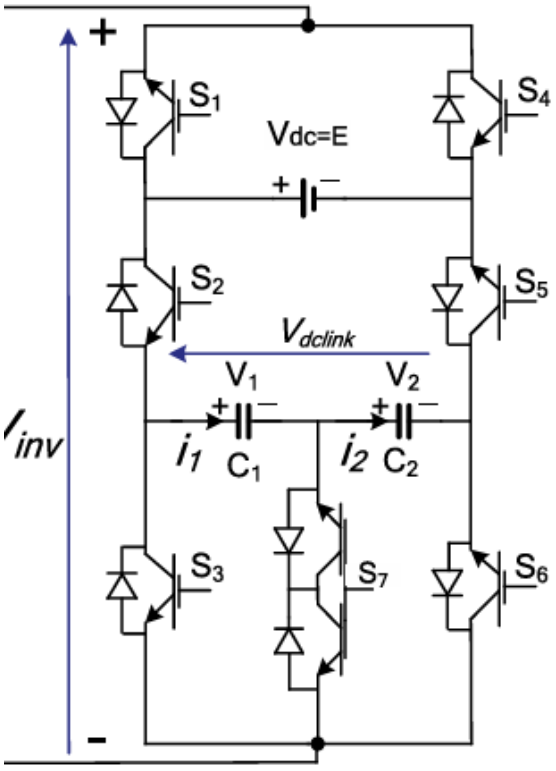

Figure 2.12: Single-phase PEC Inverter.

The possible states of PEC9 switching and states of capacitors voltages are summarized in Table 2.2. The switches (S1, S4), (S2, S5) and (S3, S6, S7) work in complement and twelve switching states are considered for the nine levels of voltage Vinv to the ac terminal. When Vdc = E andV1 = V2 = Vdc/4, achieving the levels of Vdc/4, ±Vdc/2, ±3Vdc/4, ±Vdc and0 [25].

Table 2.2: Switching States of PEC9 Inverter Topology(↑:CHARGING, ↓:DISCHARGING,:NOEFFECT)

State	$(\mathbf{S_1}, \mathbf{S_2}, \mathbf{S_3}, \mathbf{S_4}, \mathbf{S_5}, \mathbf{S_6}, \mathbf{S_7})$							$\mathbf{C_1}$	$\mathbf{C_2}$	$\mathbf{V_{inv}}$
1	1	0	0	0	1	1	0	–	–	$+E$
2	1	0	0	0	1	0	1	–	↑	$V_{dc} - V_2 = +3E/4$
3	1	0	1	0	1	0	0	↑	↑	$V_{dc} - V_1 - V_2 = +E/2$
4	1	1	0	0	0	1	0	↓	↓	$V_1 + V_2 = +E/2$
5	1	1	0	0	0	0	1	↓	–	$V_1 = +E/4$
6	0	0	0	1	1	1	0	–	–	0
7	1	1	1	0	0	0	0	–	–	0
8	0	0	0	1	1	0	1	–	↓	$-V_2 = -E/4$
9	0	0	1	1	0	0	0	↓	↓	$-V_1 - V_2 = -E/2$
10	0	1	0	1	0	1	0	↑	↑	$-V_{dc} + V_1 + V_2 = -E/2$
11	0	1	0	1	0	0	1	↑	–	$-V_{dc} + V_1 = -3E/4$
12	0	1	1	1	0	0	0	–	–	$-V_{dc} = -E$

The output-generated voltage of the inverter can be written as:

$$V_{inv} = S_a V_{dc} + S_b V_1 + S_c V_2 \tag{2.7}$$

where V_{inv} is the inverter output voltage, S_a, S_b, and S_c are switching states, V_{dc} is the DC link voltage, and V_1, V_2 are voltage across capacitors C1 and C2 respectively. [25].

where:

$$S_a = S_1 - S_2 \tag{2.8}$$

$$S_b = S_2 - S_3 \tag{2.9}$$

$$S_c = \begin{cases} S_6 - S_5, & \text{if positive half-cycle} \\ S_5 - S_6, & \text{if negative half-cycle} \end{cases} \tag{2.10}$$

Table 2.3: Switching States and Voltage Levels of the PEC Inverter

state	**Sa**	**Sb**	**Sc**	**C1**	**C2**	**Vinv**
1	1	0	0	No effect	No effect	+E
2	1	0	-1	No effect	charging	$+3E/4$
3	0	-1	-1	charging	charging	$+E/2$
4	0	1	1	Discharging	No effect	$+E/2$
5	0	1	0	Discharging	No effect	$+E/4$
6	0	0	0	No effect	No effect	0
7	0	0	0	No effect	No effect	0
8	0	0	1	No effect	Discharging	$-E/4$
9	0	-1	1	Discharging	Discharging	$-E/2$
10	-1	1	-1	Discharging	charging	$-E/2$
11	-1	1	0	charging	No effect	$-3E/4$
12	-1	0	0	No effect	No effect	-E

The PEC9 inverter topology includes two capacitors in the DC-link, each ideally balanced to one-quarter of the DC source voltage. The redundant switching states enable active balancing by selecting switching configurations that charge or discharge the capacitors as needed to keep their voltages equal and stable. This balance is done dynamically during normal operation without additional control loops or sensors dedicated to voltage balancing [25], the different states of the converter and the resultant multi voltage level are shown in figure 2.13.

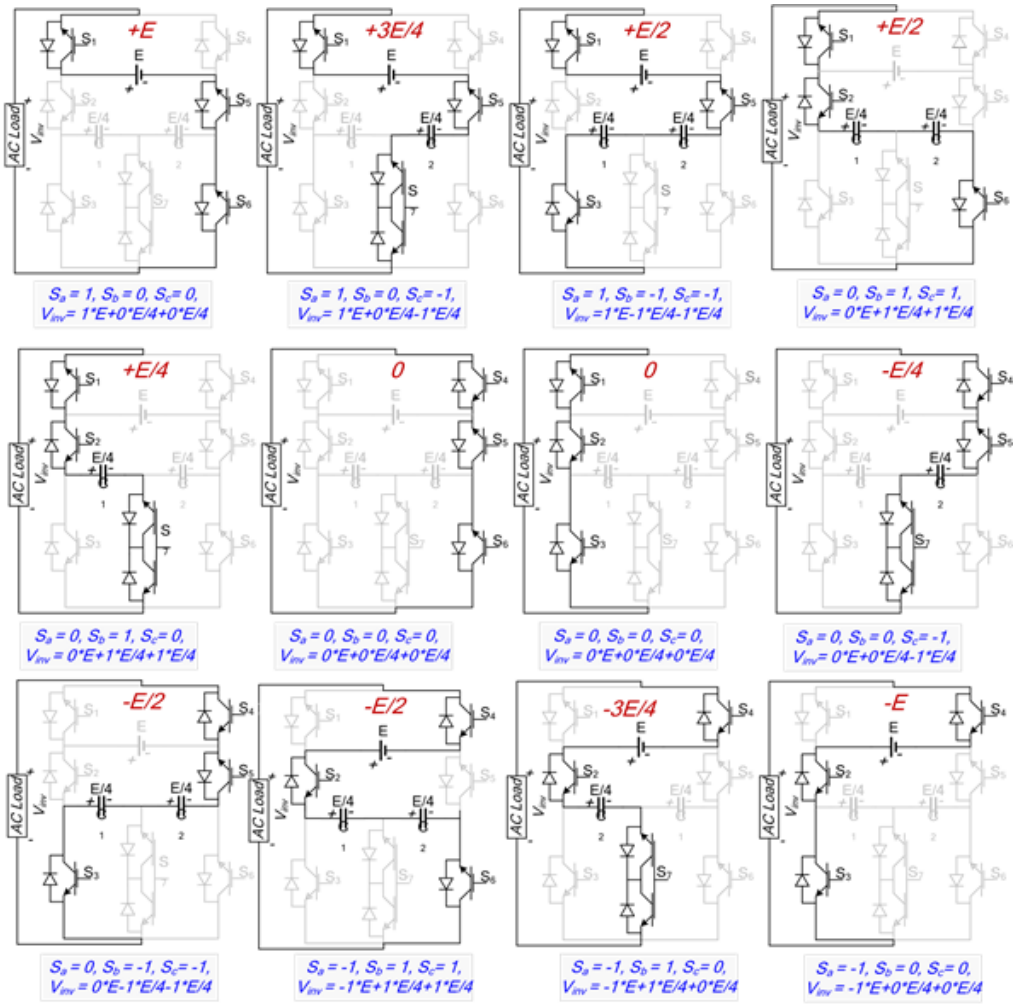

Figure 2.13: PEC9 configuration, switching states and conducting paths

2.11 Synchronization

Synchronization is a necessary condition to enable the PEC9 inverter to operate efficiently and stably while connected to the utility grid. Synchronization requires the inverter output voltage to match utility grid voltage frequency, phase and magnitude. A PLL is used to accurately extract the phase angle of the grid voltage in real-time, which will then allow for a synchronized current reference that will resemble the same properties of supply by the utility grid. The inverter control system is based on a Finite-set Model Predictive Control (FS-MPC) algorithm uses this current reference to predict the optimal switching state from the PEC9 possible states before switching to a state, while injecting current is synchronized with the grid with a low harmonic distortion and an appropriate (usually unity) power factor [25].

2.12 Non-Linear Loads

In power systems, nonlinear loads contribute switching phenomena, causing the current waveform distortion. The content of the distortion includes harmonic frequency components that are integer multiples of the frequency, and have been identified as significant contributors to a decline in power quality . Power electronic components are generally responsible for generating non-sinusoidal currents, leading to voltage waveform distortion as well . There is an increased prevalence of nonlinear loads in modern power systems, which leads to increase harmonic distortion and the reactive power demand. These conditions can negatively influence voltage stability and effectively decrease the efficiency of the electrical system. Additionally, active power filters (APFs) are routinely used to provide harmonic compensation and reactive power adequacy, in order to comply with power quality regulations [7]

2.13 Filters

Power rectifiers are typically used in industrial applications to convert AC power into DC power for many other electrical loads. As rectifiers behave as nonlinear loads, they carry harmonic currents back into the AC supply; therefore, they will create other effects in the power grid and the electrical supply. Quite a few different methods have been developed to mitigate such harmonic effects including passive L filters and active power filters (APFs), which also are now being installed more often in order to improve power quality [26].

2.13.1 L Passive Filters

Passive harmonic filters typically use Inductors (L), Capacitors (C), and Resistors (R). They can be wired in series, parallel, or a combination of the two so that proper filtering will occur. Passive filters aim to reduce harmonic distortion by using inductive and capacitive values that resonate at certain harmonic frequencies allowing filtering to occur in a power system exhibiting harmonic resonance at that frequency. Passive harmonic filters are used to improve power quality for their simple design and relatively low cost [27].

Filters are named according to the frequency range of signals that they let pass through

while blocking the rest, where:

- **Low-Pass Filter (LPF):** Accepts signals from 0 Hz to the cutoff frequency and blocks signals at higher frequencies.
- **High-Pass Filter (HPF):** Accepts signals higher than the desired cut-off frequency while blocking lower frequencies.
- **Band-Pass Filter (BPF):** Allows signals to pass only if they fall within the desired frequency range, blocking frequencies outside this range.

Filters are also classified by their order, the order of a passive filter is an integer number, is determined by the number of used elements, also called the number of poles. In general, the higher the order of the filter, the more closely in approximates an ideal filter and the complex the circuitry required to construct it (Figures 2.14 and Figure 2.15).

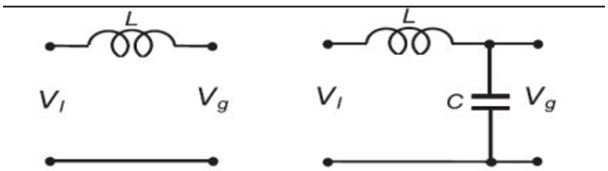

Figure 2.14: First order low pass filter and second order low pass filter

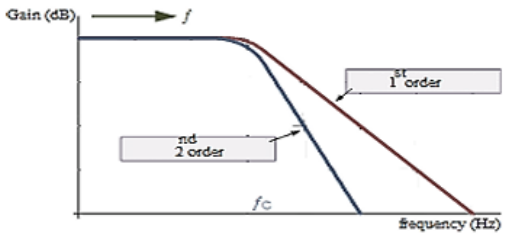

Figure 2.15: Frequency response of 1st order and 2nd order low pass filter

2.13.2 Active Power Filters

Active Power Filters (APFs) are increasingly being integrated into grid-connected photovoltaic (PV) systems by assigning this functionality to the grid-interfacing inverter. This dual-purpose approach enables the inverter not only to inject active power from the PV source into the grid but also to compensate for power quality issues such as harmonics and reactive power. Typically, APF operation requires an external power source and utilizes

passive components like resistors and capacitors, while avoiding inductors to maintain a compact, cost-effective, and efficient design [7].

In such systems, a device that integrates an inverter and a solar panel can act as an APF. This setup operates within a power system composed of a three-phase source and nonlinear loads. The most commonly adopted APF configurations include series, shunt, and hybrid types .

- The **series active power filter (SAPF)** is connected through a coupling transformer and injects a compensating voltage in series with the supply voltage to eliminate voltage harmonics [28] as shown in figure 2.16,a.
- The **shunt active power filter** detects harmonic components of the load current and injects compensating currents at the point of common coupling (PCC), thereby mitigating harmonics and reactive power as shown in figure 2.16.b. This ensures that the source current remains sinusoidal [29].
- The **hybrid active power filter** integrates both series and shunt configurations, along with passive filters, to enhance harmonic mitigation and improve overall system stability [30].

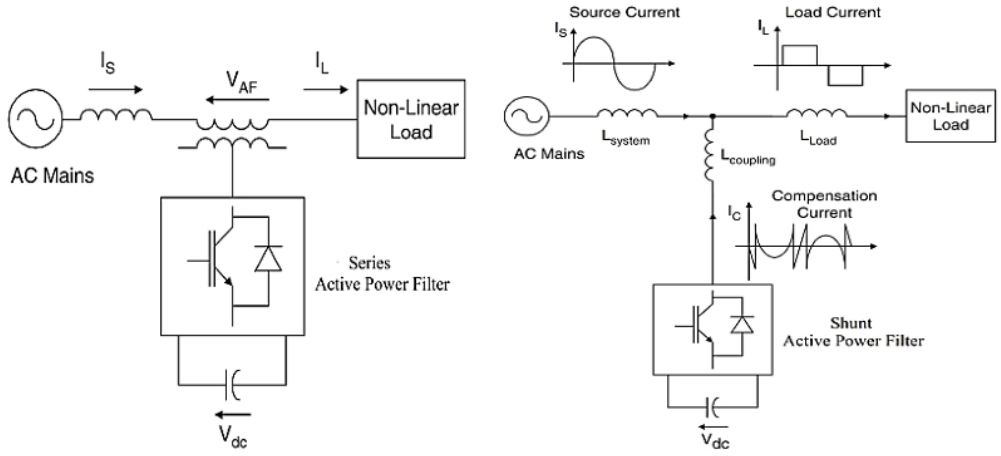

a) Series active power filter b) Shunt active power filter

Figure 2.16: Active power filters

2.14 Conclusion

The modeling of the Solar-AF system has been presented, covering key stages including photovoltaic power generation, maximum power point tracking (MPPT), DC-AC inversion using PEC9, and active filtering. The following chapter will focus on the control strategies employed to ensure optimal performance and stability of the system.

CHAPTER 3

System Control Design

3.1 Introduction

The proposed Solar Active Power Filter (SAPF) system is designed to mitigate harmonic currents, improve power factor, peak power extraction from a photovoltaic (PV) array, reactive power compensation and maintain DC-link voltage stability under dynamic load conditions. It operates by injecting compensating current into the grid to counteract the distortions introduced by the nonlinear load. The use of a multilevel inverter, specifically the nine-level Packed E-Cell (PEC9) inverter, enhances the quality of the injected current by reducing switching losses and total harmonic distortion (THD) compared to conventional two-level inverters.

In the implemented control system, the DC-DC converter control necessitates PV array voltage and PV current as inputs, while the generation of reference compensating currents requires real-time measurements of load currents, grid voltage at the point of common coupling (PCC), and the DC-link capacitor voltages. The inverter switching strategy is determined based on these reference currents and the state of the capacitors to ensure voltage balancing and accurate harmonic compensation.

The control approach developed for the PEC9 inverter is presented in this chapter. The effectiveness of this control is evaluated on the basis of the grid current quality and the ability to maintain the desired voltage across the DC link capacitors stable and obtain the desired voltage levels at the inverter output.

3.2 System Configuration

3.2.1 Grid connected Configuration

The proposed configuration of the single-phase nine-level Packed E-Cell (PEC9) inverter, along with the developed finite-set model predictive control (FS-MPC) scheme. The investigated system consists of a single-phase AC source connected to an RL load through the PEC9 inverter output terminals as illustrated in Figure3.1. The main objective of the FS-MPC strategy is to regulate the grid current and balance the DC-link capacitor voltages, and ensuring low total harmonic distortion (THD) [31].

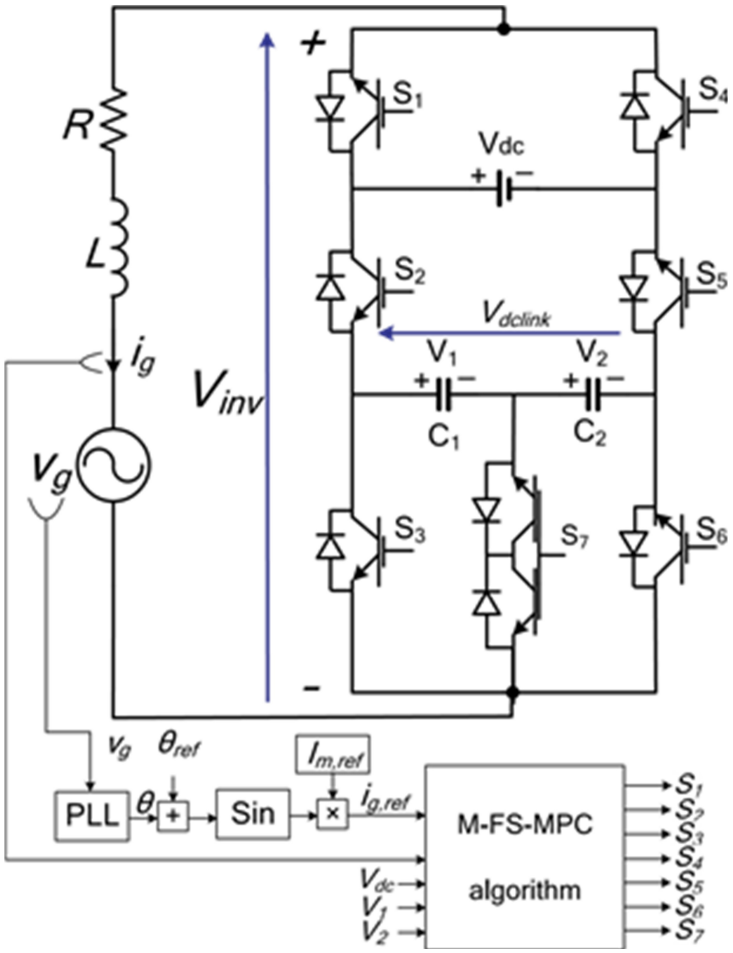

Figure 3.1: Grid connected Packed E-cell inverter

3.2.2 PEC9 Based active filter Configuration

The grid-connected configuration of the proposed single-phase nine-level Packed E-Cell (PEC9) inverter, operating as a shunt solar active power filter (SAF), is illustrated in Figure 3.2. The system under study consists of an AC source, a nonlinear load, and the PEC9 inverter, which is connected in parallel to the grid through a series RL filter ($R_f L_f$) at the point of common coupling (PCC). The system is designed to inject the extracted solar power—delivered by a photovoltaic (PV) array through a boost converter—into the grid via the DC-link capacitor of the PEC9 inverter, while simultaneously performing active filtering functions. The implemented finite set model predictive control (FS-MPC) algorithm ensures accurate reference current tracking, effective harmonic mitigation, and dynamic compensation of reactive power under varying load and source conditions.

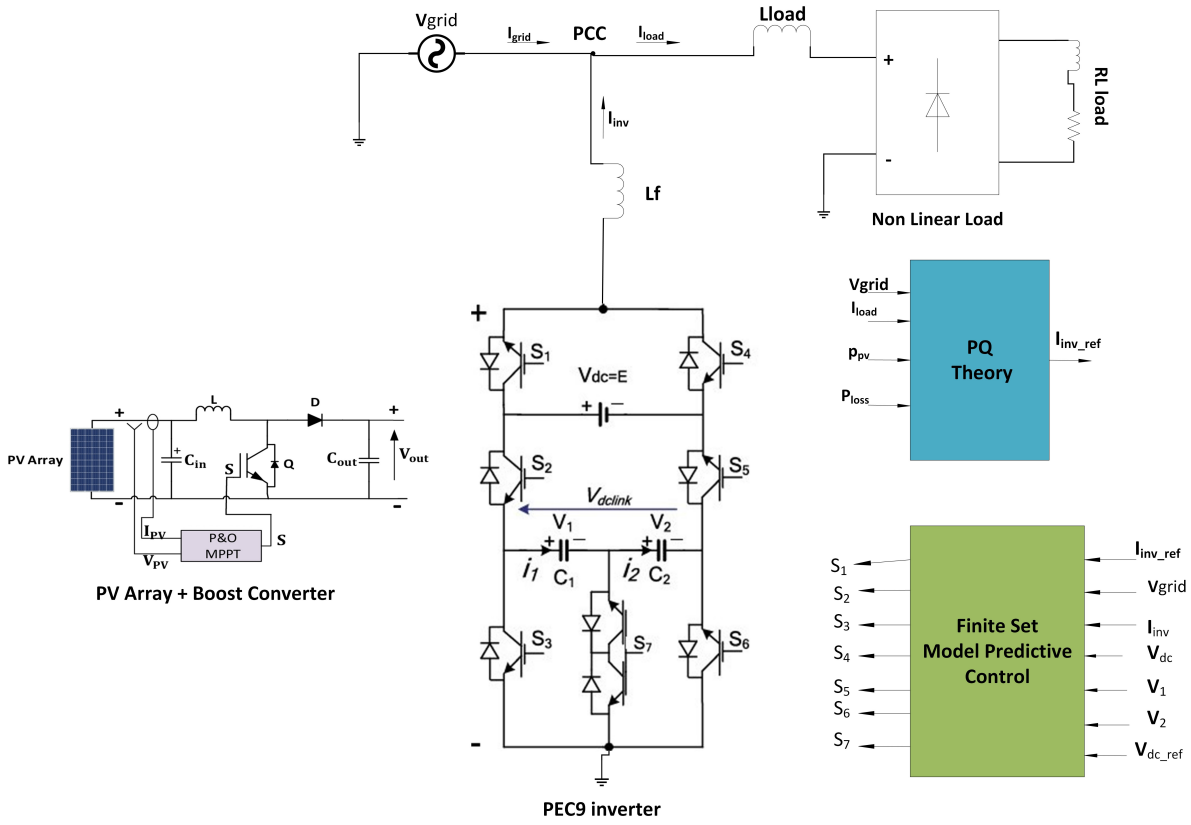

Figure 3.2: PEC9 Based solar active filter

3.3 PQ Theory

In 1983, Akagi et al. [32] introduced the "Generalized Theory of the Instantaneous Reactive Power in Three-Phase Circuits," commonly referred to as the instantaneous power theory or p-q theory. This theory is formulated using instantaneous values of voltages and currents in three-phase power systems, with or without a neutral conductor, and is applicable under both steady-state and transient operating conditions. It remains valid regardless of the waveform shape, making it suitable for systems with nonsinusoidal signals. The p-q theory involves an algebraic transformation—specifically, the Clarke transformation—that converts the three-phase quantities in the a-b-c coordinate system into the α, β,0 coordinate system. This is followed by the computation of instantaneous real and imaginary power components, which serve as the basis for various control strategies in active power filtering [33].

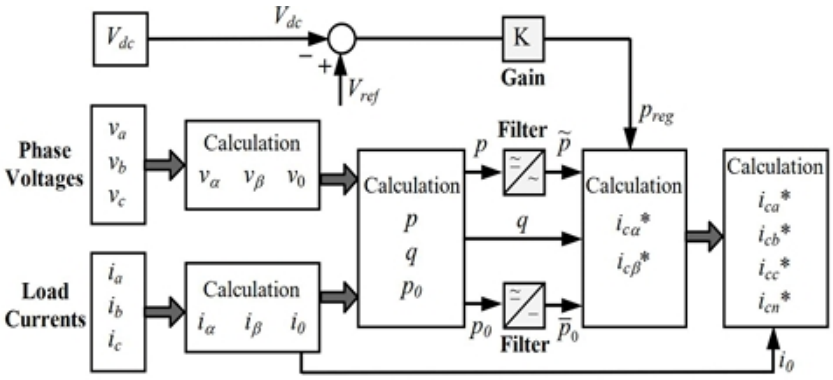

Figure 3.3: Calculations for the constant instantaneous supply power control strategy

Instantaneous power components are computed as follows :

$$\begin{bmatrix} v_0 \\ v_\alpha \\ v_\beta \end{bmatrix} = \sqrt{\frac{2}{3}} \begin{bmatrix} 1/\sqrt{2} & 1/\sqrt{2} & 1/\sqrt{2} \\ 1 & -1/2 & -1/2 \\ 0 & \sqrt{3}/2 & -\sqrt{3}/2 \end{bmatrix} \begin{bmatrix} v_a \\ v_b \\ v_c \end{bmatrix} \quad \begin{bmatrix} i_0 \\ i_\alpha \\ i_\beta \end{bmatrix} = \sqrt{\frac{2}{3}} \begin{bmatrix} 1/\sqrt{2} & 1/\sqrt{2} & 1/\sqrt{2} \\ 1 & -1/2 & -1/2 \\ 0 & \sqrt{3}/2 & -\sqrt{3}/2 \end{bmatrix} \begin{bmatrix} i_a \\ i_b \\ i_c \end{bmatrix} \tag{3.1}$$

If the system is three-phase with three wires, there are no zero sequence current components (no neutral conductor), so i_0 can be removed from the above equations, simplifying them. The current analysis will concentrate on three-wire systems. As a result, there is no zero-sequence voltage or current [34]. The power components p and q are related to the same α, β voltages and currents, and can be written together as :

$$\begin{bmatrix} p \\ q \\ p_0 \end{bmatrix} = \begin{bmatrix} v_\alpha & v_\beta & 0 \\ v_\beta & -v_\alpha & 0 \\ v_0 & 0 & 0 \end{bmatrix} \begin{bmatrix} i_\alpha \\ i_\beta \\ i_0 \end{bmatrix} \tag{3.2}$$

These quantities are illustrated in Figure 3.4 for an electrical system represented in a-b-c coordinates and have the following physical meaning :

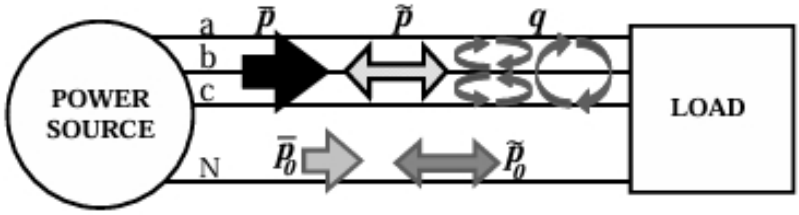

Figure 3.4: Power components of the p-q theory in a-b-c coordinates

$\bar{p_0}$ = Mean value of the instantaneous zero-sequence power – corresponds to the energy

per time unity which is transferred from the power supply to the load through the zero-sequence components of voltage and current.

$\tilde{p_0}$= Alternated value of the instantaneous zero-sequence power – it means the energy per time unity that is exchanged between the power supply and the load through the zero-sequence components.

$\bar{p}$ = Mean value of the instantaneous real power – corresponds to the energy per time unity which is transferred from the power supply to the load, through the a-b-c coordinates, in a balanced way (it is the desired power component).

$\tilde{p}$ = Alternated value of the instantaneous real power – It is the energy per time unity that is exchanged between the power supply and the load, through the a-b-c coordinates.

q = Instantaneous imaginary power – corresponds to the power that is exchanged between the phases of the load. In the case of a balanced sinusoidal voltage supply and a balanced load, with or without harmonics, $\bar{q}$ (the mean value of the instantaneous imaginary power) is equal to the conventional reactive power ($\bar{q} = 3 \cdot V \cdot I_1 \cdot sin\phi_1$) [33].

3.3.1 The p-q Theory Applied to Shunt Active Filters

As previously discussed, the active component $\bar{p}$ is typically the only desirable power quantity in the p–q theory. The remaining components, including the oscillating and zero-sequence powers, can be effectively compensated using a shunt active power filter as illustrated in Figure 3.5. According to Watanabe et al. [35, 36], the zero-sequence power component $\bar{p_0}$ can be compensated without requiring an external power source within the filter itself. Instead, this power is redirected from the source to the load through the active filter.This means that the energy previously transferred from the source to the load through the zero-sequence components of voltage and current, is now delivered in a balanced way from the source phases [33]

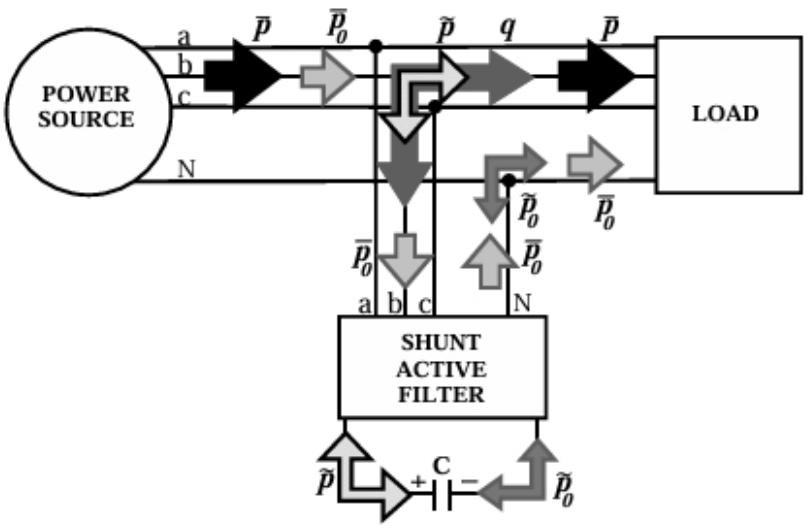

Figure 3.5: Compensation of power components $\tilde{p}$,q,$\tilde{p_0}$ and $\bar{p_0}$ in a-b-c coordinates

Then to calculate the reference compensation currents in the α-β coordinates, expression (3.2) is inverted, and the powers to be compensated ($\tilde{p}$,$\bar{p_0}$, and q) are used:

$$\begin{bmatrix} i^*_{c\alpha} \\ i^*_{c\beta} \end{bmatrix} = \frac{1}{v_\alpha^2 + v_\beta^2} \cdot \begin{bmatrix} v_\alpha & -v_\beta \\ v_\beta & v_\alpha \end{bmatrix} \cdot \begin{bmatrix} \tilde{p} - \bar{p}_0 \\ q \end{bmatrix} \tag{3.3}$$

Since the zero-sequence current must be compensated, the reference compensation current in the coordinate is i_0 itself:

$$i_{c0} = i_0 \tag{3.4}$$

In order to obtain the reference compensation currents in the a-b-c coordinates the inverse of the transformation given in expression (3.1) is applied:

$$\begin{bmatrix} i^*_{ca} \\ i^*_{cb} \\ i^*_{cc} \end{bmatrix} = \sqrt{\frac{2}{3}} \cdot \begin{bmatrix} 1/\sqrt{2} & 1 & 0 \\ 1/\sqrt{2} & -1/2 & \sqrt{3}/2 \\ 1/\sqrt{2} & -1/2 & -\sqrt{3}/2 \end{bmatrix} \begin{bmatrix} i^*_{c0} \\ i^*_{c\alpha} \\ i^*_{c\beta} \end{bmatrix} \tag{3.5}$$

$$i^*_{cn} = -(i^*_{ca} + i^*_{cb} + i^*_{cc})$$

3.4 Modified PQ Theory for Power Injection

The theory of instantaneous reactive power remains one of the most robust and widely adopted techniques for generating instantaneous reference signals in active power filtering applications. Originally designed for three-phase systems,including both three- and four-wire configurations [37].This method has since been extended to address the demands of single-phase systems. Moreover, in scenarios involving unbalanced supply voltage and/or load conditions, the single-phase 'p-q' theory demonstrates the capability to generate a sinusoidal source current and efficiently manage multi-phase systems, surpassing the performance of the three-phase theory [38].

The core principle of the single-phase p–q theory lies in shifting the initial system voltage and current by $\pi/2$ in either direction, creating a pseudo-two-phase system. This approach facilitates the expression of the entire system in α-β coordinates, where α-axis values correspond to the initial source voltage and load current, and β-axis quantities result from the displacement of the source voltage and load current by$\pi/2$ [39, 40].

The representation of single-phase source voltage involves a $\pi/2$ forward shift in α-β coordinates .

$$\begin{bmatrix} V_\alpha(\omega t) \\ V_\beta(\omega t) \end{bmatrix} = \begin{bmatrix} V_{grid}(\omega t) \\ V_{grid}\left(\omega t + \frac{\pi}{2}\right) \end{bmatrix} \tag{3.6}$$

In the same way, the load current representation in a coordinate system with a $\pi/2$ forward shift.

$$\begin{bmatrix} I_\alpha(\omega t) \\ I_\beta(\omega t) \end{bmatrix} = \begin{bmatrix} I_{load}(\omega t) \\ I_{load}\left(\omega t + \frac{\pi}{2}\right) \end{bmatrix} \tag{3.7}$$

The power components 'p' and 'q' can be represented together since they are related to the same α-β voltages and currents.

$$\begin{bmatrix} p(\omega t) \\ q(\omega t) \end{bmatrix} = \begin{bmatrix} V_\alpha(\omega t) & V_\beta(\omega t) \\ -V_\beta(\omega t) & V_\alpha(\omega t) \end{bmatrix} \cdot \begin{bmatrix} I_\alpha(\omega t) \\ I_\beta(\omega t) \end{bmatrix} \tag{3.8}$$

The expressions for the $p(\omega t)$ and $q(\omega t)$ are:

$$p(\omega t) = \bar{p}(\omega t) + \tilde{p}(\omega t) \tag{3.9}$$

$$q(\omega t) = \bar{q}(\omega t) + \tilde{q}(\omega t) \tag{3.10}$$

The instantaneous fundamental active and reactive power is represented by the DC components $\bar{p}(\omega t)$and $\bar{q}(\omega t)$,while the harmonic power is represented by the AC components $\tilde{p}(\omega t)$ and $\tilde{q}(\omega t)$. In the following, the AC component (($\tilde{p}(\omega t)$)) of active power and the overall reactive power ($q(\omega t)$) are employed for computing the harmonic reference current [39].

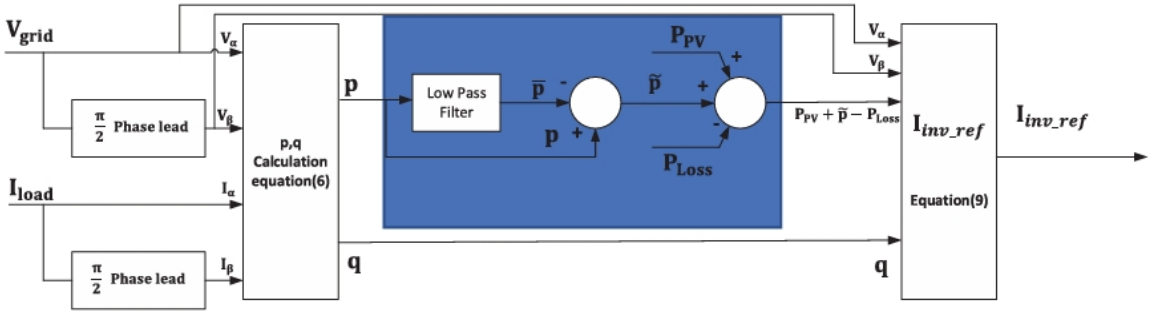

Figure 3.6: Modified p-q power injection

To counterbalance voltage source inverter switching losses and maintain the desired DC-link voltage, the shunt active power filter draws a minimal amount of real power (P_{loss}) either from the single-phase AC source or an external power source.

In addition to reducing harmonics, it will provide active power from the PV array connected via a boost converter to the inverter.To inject this power into the grid,we thus updated the PQ theory and included the PV power with the AC component ($p(\omega t)$) of active power.Therefore,as seen in Figure 3.6, we need a particular feedback signal to force the control circuit to include power and harmonics in its output [39].The reference compensating current can be obtained by this equation:

$$I_{inv\_ref} = \frac{((V_\alpha \times (P_{PV} + \tilde{p} - P_{Loss})) - V_\beta \times q)}{V_\alpha^2 + V_\beta^2} \tag{3.11}$$

3.5 Conventional Single Phase Two Level Inverter

Following the discussion on the p–q theory and reference current generation, this section introduces the conventional two-level single-phase inverter, which serves as the core power conversion stage in the active filtering system. This inverter is responsible for injecting compensating currents into the grid based on the reference signals. To ensure accurate and stable operation, appropriate control strategies are applied to regulate the output voltage

and track the reference current waveform. In the subsequent sections, different control techniques including voltage regulation method, Hysteresis Current Control (HCC), and Model Predictive Control (MPC) are explored in the context of single-phase inverter operation.

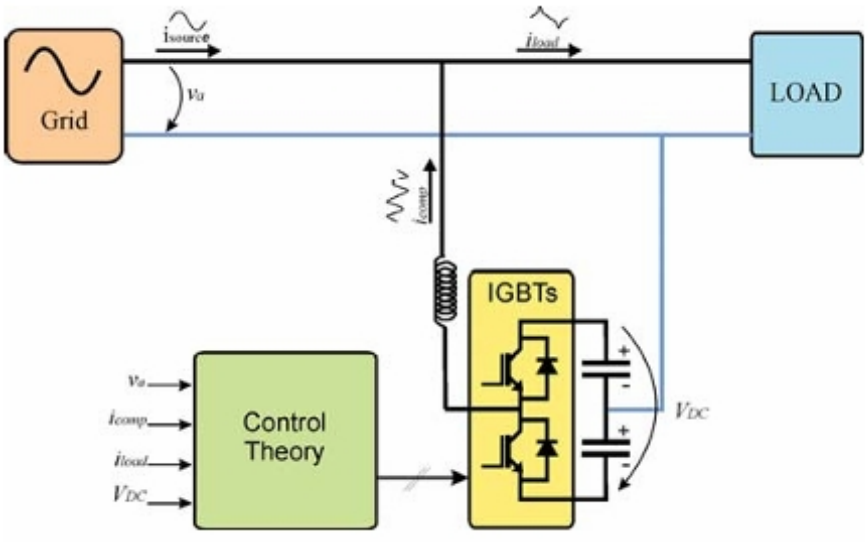

Figure 3.7: Block Diagram of the Single-Phase Active Power Filter.

3.5.1 Voltage Regulation

Voltage regulation plays a critical role in maintaining the stability and performance of the voltage value at the capacitors in the DC side of the power inverter. A stable DC-link voltage ensures that the inverter can continuously deliver the required compensating current to the grid without interruption [41].

The value of P_{loss} is determined by means of a PI controller that eliminates the error between the DC-link voltage and the. It is important to explain that during the normal operation of the SAPF, the soft-power oscillating value components defined by p-q theory are exchanged between the loads and the DC link capacitors of the SAPF, and therefore it is natural for the DC link capacitors to oscillate to compensate for these power components [42].

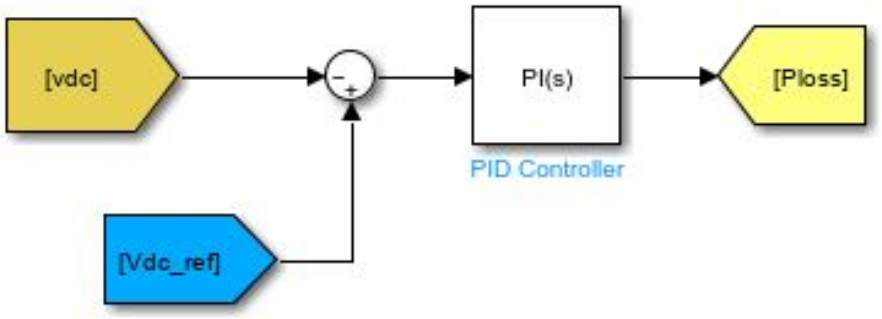

Figure 3.8: DC voltage regulation

3.5.2 Hysteresis Current Control (HCC)

Hysteresis Current Control (HCC) is a widely adopted technique used nonlinear control for current-regulated inverters.It's schemes are based on a nonlinear feedback loop with two level hysteresis comparators, it makes sure that sensed grid currents follow reference grid currents. As is Figure 3.9 shows [43].

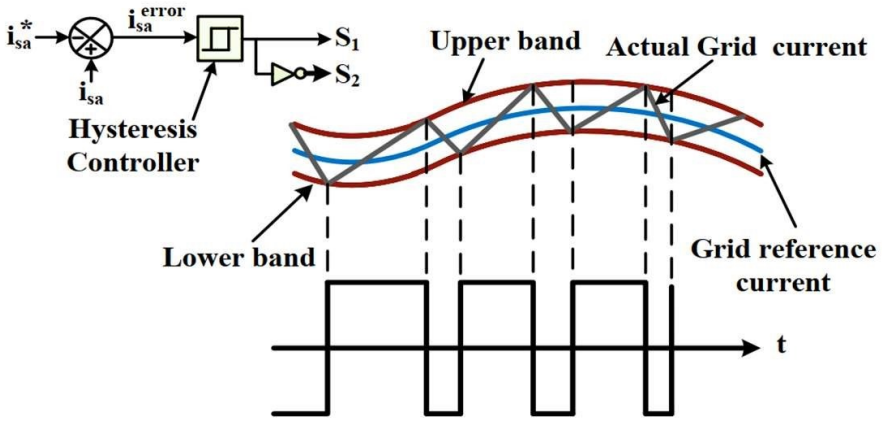

Figure 3.9: Description of the hysteresis current controller

The switching signals S1 and S2 are produced directly when the error exceeds an assigned tolerance band HB. such that:

- If $i_{sa}^{error} < HB$, the upper switch S1 is off and the lower switch S2 is on.
- If $i_{sa}^{error} > HB$, the upper switch S1 is on and the lower switch S2 is off.

Note that the upper band and the lower band differ by $2HB$.

With this method, the actual current is forced to follow a reference current within a specified hysteresis band. The inverter current is sensed in real time and compared to

reference current to generate switching pulses to switch on and off the inverter IGBTs. If the current exceeds the upper level of the band, then the inverter upper switch is switched off and the lower switch is switched on. Conversely, if the current is below the lower hysteresis limit, the inverter upper switch is switched on and the lower switch is switched off. This switching action provides accurate current tracking and compensation of harmonics and reactive power [44]

3.5.3 Model Predictive Control (MPC)

MPC is a sophisticated, advanced ,and effective control technique than traditional PID and HCC control, to control the power converters. It is based on the mathematical model of the studied system in order to predict the future behavior of the controlled variables. Then, to form these predictions, a cost function is defined and evaluated in order to select the optimal control action [45]. At each sampling instant, the controller evaluates all possible switching states of the inverter and uses the system model to forecast the next-step output current.

The flowchart in Figure 3.10 illustrates the functionality of the suggested MPC.

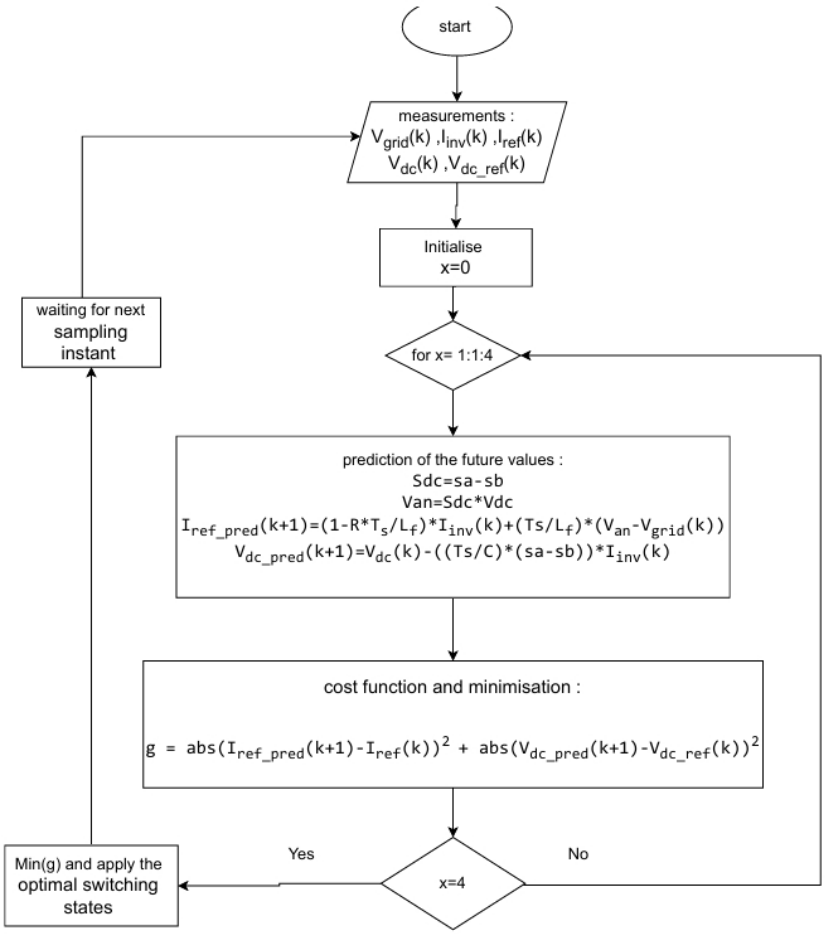

Figure 3.10: MPC for single phase conventional APF

For each of the four switching states,the inverter current I_{inv} measured values, grid voltage V_{grid}, and capacitor voltage V_{dc} are used to calculate the future values of the reference current $I_{refpred}$ and the capacitor voltage V_{dcpred}. The cost function (g) incorporates these control goals in the following function:

$$g = \text{abs}(I_{\text{ref\_pred}}(k+1) - I_{\text{ref}}(k))^2 + \text{abs}(V_{\text{dc\_pred}}(k+1) - V_{\text{dc\_ref}}(k))^2 \tag{3.12}$$

3.6 Packed E-Cell Single Phase Inverter (PEC9)

The proposed PEC9 structure is constituted by one dc source Vdc, two capacitors C1 and C2 horizontally extended to form a single auxiliary dc link, six active power switches noted as S1,S2,S3,S4,S5, and S6 and one bidirectional switch noted as S7 .This latter is connected between the capacitors midpoint and PEC9 ac terminal [25].

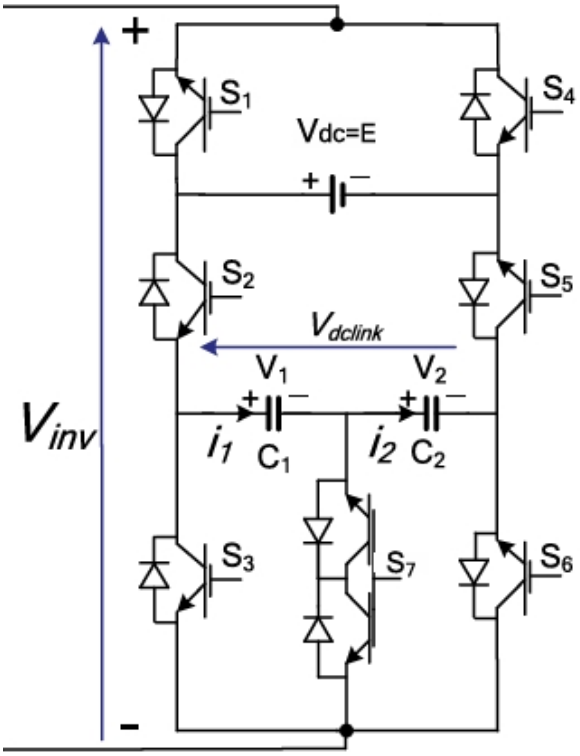

Figure 3.11: PEC9 inverter topology

To generate nine-level voltage at the inverter output the voltage across the capacitors V_{C1} and V_{C2} should be balanced to one quarter of the input DC voltage magnitude E. While, the sum of capacitor voltages V_{C1} and V_{C2} is regulated to the magnitude of input DC voltage E, as presented in the table below 12 possible switching states can produced by the PEC9 to generate nine level voltage [25].

When a fault occurs on the bidirectional switch S7, the PEC9 inverter will be operating as PUC operation as the previous generation of the compact multilevel inverter, where five and seven levels can be achievable.

Table 3.1: Switching States of PEC9 Inverter Topology(↑:CHARGING, ↓:DISCHARGING,:NOEFFECT)

State	$(S_1, S_2, S_3, S_4, S_5, S_6, S_7)$							C_1	C_2	V_{inv}
1	1	0	0	0	1	1	0	–	–	$+E$
2	1	0	0	0	1	0	1	–	↑	$V_{dc} - V_2 = +3E/4$
3	1	0	1	0	1	0	0	↑	↑	$V_{dc} - V_1 - V_2 = +E/2$
4	1	1	0	0	0	1	0	↓	↓	$V_1 + V_2 = +E/2$
5	1	1	0	0	0	0	1	↓	–	$V_1 = +E/4$
6	0	0	0	1	1	1	0	–	–	0
7	1	1	1	0	0	0	0	–	–	0
8	0	0	0	1	1	0	1	–	↓	$-V_2 = -E/4$
9	0	0	1	1	0	0	0	↓	↓	$-V_1 - V_2 = -E/2$
10	0	1	0	1	0	1	0	↑	↑	$-V_{dc} + V_1 + V_2 = -E/2$
11	0	1	0	1	0	0	1	↑	–	$-V_{dc} + V_1 = -3E/4$
12	0	1	1	1	0	0	0	–	–	$-V_{dc} = -E$

3.7 Perturb and Observe Method

The Perturb and Observe (P and O) algorithm is among the most commonly used methods for maximum power point tracking (MPPT) in photovoltaic (PV) systems, primarily due to its simplicity and ease of implementation. The algorithm functions by periodically perturbing the terminal voltage of the PV module and comparing the resulting output power with that of the previous perturbation cycle. As shown in Figure 3.11, if the change in voltage leads to an increase in power, the control system continues to shift the operating point in the same direction. Conversely, if the power decreases, the direction of perturbation is reversed. The flowchart representing the P and O algorithm is depicted in Figure 3.11 [46].

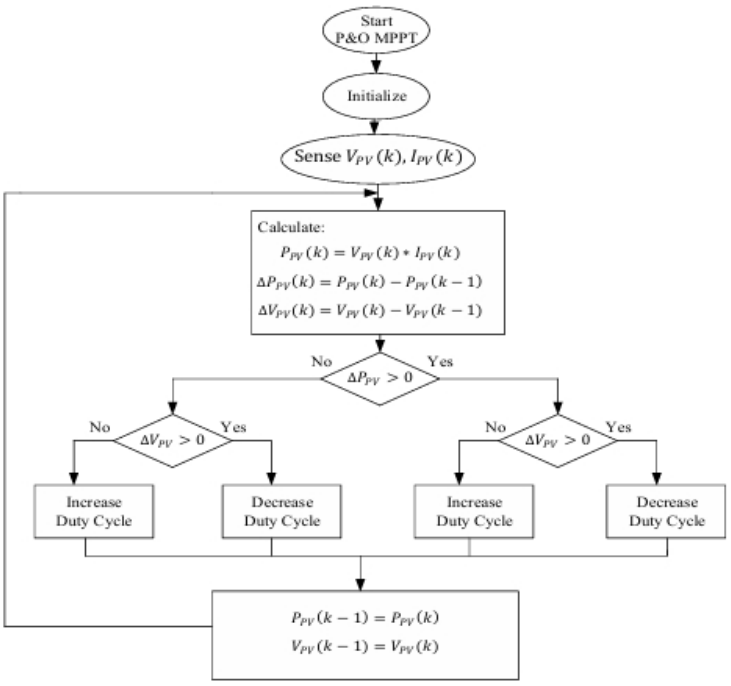

Figure 3.12: The P and O method flowchart

3.8 Finite Set MPC (FS-MPC) for PEC9

Finite Set-MPC is one of the major categories of MPCs. FS-MPC is a simple, intuitive, and very flexible control technique that can be appropriately implemented on power converters. Moreover,this method allows the inclusion of system nonlinearities and constraints in the controller design. The main idea behind this technique is the use of the inherent discrete nature of power converter for the prediction of future behavior of the variables to control for a predefined time horizon [25].

It selects the appropriate switching state that minimizes a defined cost function at each sampling instant. The cost function is formulated to reflect the control objectives that need to be achieved optimally. One of the main advantages of Finite Set Model Predictive Control (FS-MPC) is that it eliminates the need for a separate modulator, as the switching pulses are directly applied to the converter.

3.8.1 FS-MPC For Grid Connected PEC9 converter

The design of the FS-MPC control technique for the Grid Connected PEC9 inverter focuses on controlling three main variables: the line current i_g injected into the utility

grid, and the voltages across the two DC-link capacitors V_1 and V_2. Accordingly, the switching variables S_a, S_b and S_c as defined in Table 2.1, are treated as the system's control inputs or state variables [25].

$$V_{inv} = S_a V_{dc} + S_b V_1 + S_c V_2 \tag{3.13}$$

As mentioned before, if the two dc-link capacitor voltages are regulated to one-fourth of the dc voltage source, the output voltage wave form Vinv contains nine voltage levels. The dynamic model of the inverter grid side is described as follows

$$L\frac{di_g}{dt} = -Ri_g + V_{\text{inv}} - v_g \tag{3.14}$$

A discrete-time model has to be taken into consideration where T_s is the system sampling time. Adapting Euler-forward approximation, the line current derivative is written as follows:

$$\frac{di_g(t)}{dt} = \frac{i_g(k+1) - i_g(k)}{T_s} \tag{3.15}$$

Substituting (3.3) into (3.2) leads to the following equation:

$$i_g(k+1) = \left(1 - \frac{RT_S}{L}\right) i_g(k) + \frac{T_s}{L_g}(V_{\text{inv}}(k) - v_g(k)) \tag{3.16}$$

Concerning the dc-side voltages V_1 and V_2 across the capacitors C_1 and C_2,respectively

$$i_1 = C_1\frac{dV_1}{dt} = -S_b i_g \tag{3.17}$$

$$i_2 = C_2\frac{dV_2}{dt} = -S_c i_g \tag{3.18}$$

Using Euler-forward approximation, each capacitor voltage $V_i, i = (1, 2)$ is written as

$$\frac{dV_i(t)}{dt} = \frac{V_i(k+1) - V_i(k)}{T_s} \tag{3.19}$$

Substituting (3.7) in the corresponding voltage of (3.5) and (3.6), (3.8) and (3.9) are obtained, respectively

$$V_1(k+1) = V_1(k) - \frac{T_s \times S_b}{C_1} i_g(k) \tag{3.20}$$

$$V_2(k+1) = V_2(k) - \frac{T_s \times S_c}{C_2} i_g(k) \tag{3.21}$$

where Sa ,Sb and Sc are obtained from table 2.2.

Finally, the cost function g is derived as the following equation:

$$g = k_1(i_{g,\text{ref}} - i_g(k))^2 + k_2(V_{1,\text{ref}} - V_1(k))^2 + k_2(V_{2,\text{ref}} - V_2(k))^2 \tag{3.22}$$

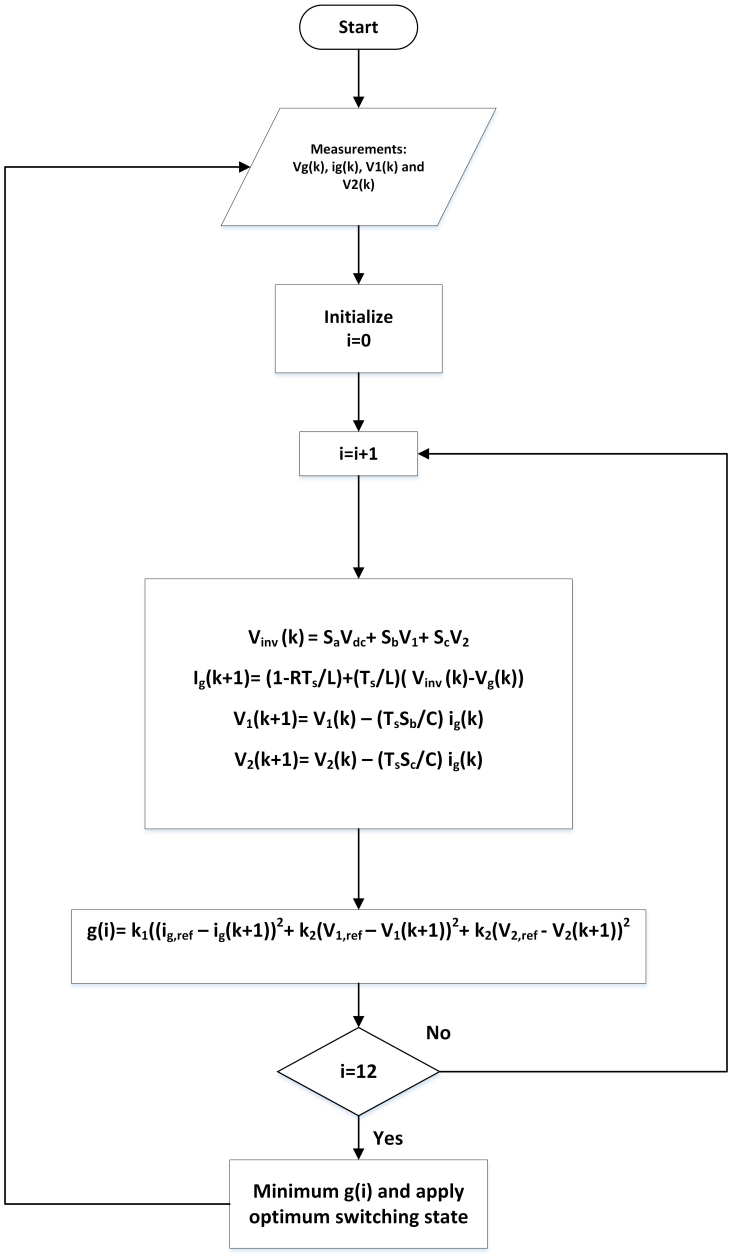

Figure 3.13: Finite Set MPC for PEC9

Figure 3.11 presents the FS-MPC flowchart implemented for the PEC9 inverter. At every sampling instant k, the system acquires the current values of the grid current $i_g(k)$ and the voltages across the two DC-link capacitors $V_1(k)$ and $V_2(k)$. Using equations (3.4),

(3.8), and (3.9), these values are used to predict the corresponding states at the next time step $k+1$. A cost function is then evaluated to quantify the deviation between the predicted values and their respective reference values [25].

The FS-MPC controller evaluates all 12 possible switching combinations of the PEC9 inverter, as defined by the switching variables S_a, S_b, and S_c in Table 2.1. The combination that results in the lowest cost function value is selected to generate the appropriate switching signals for the inverter switches S_1 to S_7, based on the logic outlined in Table 3.1. The cost function includes two weighting coefficients, k_1 and k_2, which balance the importance of each control objective. These parameters are typically tuned empirically, as there is no standard analytical method for determining their optimal values [25].

3.8.2 FS-MPC for PEC9 Converter Based Active Filter

The proposed FS-MPC strategy enables the PEC9 inverter to operate in both active power filtering and grid-connected photovoltaic (PV) injection modes. The flowchart shown in Figure 3.12 illustrates the functionality of the proposed control algorithm.

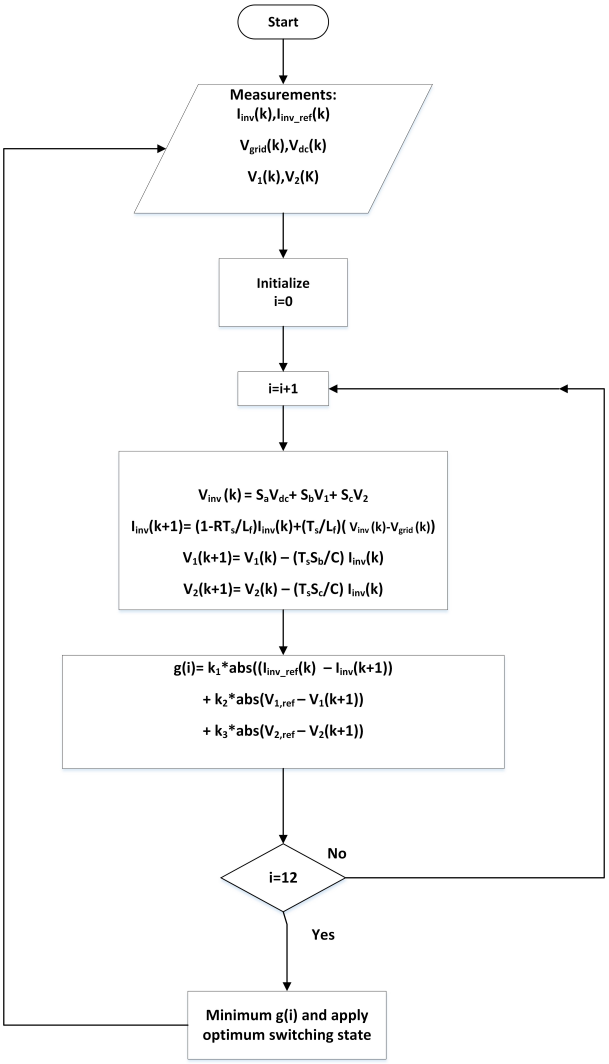

Figure 3.14: Finite Set MPC for grid PEC9 converter

For each of the 12 possible switching states, the inverter current I_{inv} is measured, and the grid voltage V_{grid} along with the DC-link capacitor voltages V_1 and V_2 are used to predict the future values of the inverter current and capacitor voltages. The core objective of this control technique is to implement predictive switching by minimizing a defined cost function g at each sampling instant k, thereby ensuring accurate reference current tracking, effective harmonic compensation, and balanced operation of the DC-link capacitors.

The cost function (g) incorporates these control goals is defined as:

$$g(i) = k_1 * \text{abs}((I_{\text{inv,ref}}(k) - I_{\text{inv}}(k+1)) + k_2 * \text{abs}(V_{1,\text{ref}} - V_1(k+1)) + k_3 * \text{abs}(V_{2,\text{ref}} - V_2(k+1)) \tag{3.23}$$

The cost function includes three weighting factors, k_1, k_2, and k_3 which balance the

importance of each control objective. These parameters are typically tuned randomly, as there is no standard analytical method for determining their optimal values.

the inverter current reference is denoted by the variable $I_{\text{inv,ref}}(k)$ with it's predicted value $I_{\text{inv}}(k+1)$, and the same for the dc-link capacitor voltages, the reference is $V_{1,\text{ref}}$ and $V_{2,\text{ref}}$ which is fourth of V_dc, and their predicted values are respectively $V_1(k+1)$, $V_2(k+1)$.

The dynamic model of the inverter grid side is described as follows:

$$L_f \frac{di_{inv}}{dt} = V_{inv} - V_{grid} \tag{3.24}$$

The filter current derivative is written as per Euler-Forward approximation, as follows:

$$\frac{di_{inv}(t)}{dt} = \frac{i_{inv}(k+1) - i_{inv}(k)}{T_s} \tag{3.25}$$

Substituting Eq. (3.13) into Eq. (3.12) gives:

$$i_{inv}(k+1) = i_{inv}(k) + \frac{T_s}{L_{inv}}(V_{inv}(k) - v_{grid}(k)) \tag{3.26}$$

The voltages across both C_1 and C_2 are given as:

$$i_1 = C_1 \frac{dV_1}{dt} = -S_b i_g \tag{3.27}$$

$$i_2 = C_2 \frac{dV_2}{dt} = -S_c i_g \tag{3.28}$$

Using Euler-Forward approximation, each capacitor voltage $V_i, i = \{1, 2\}$ is written as Eq.(3.17)

$$\frac{dV_i(t)}{dt} = \frac{V_i(k+1) - V_i(k)}{T_s} \tag{3.29}$$

Accordingly, discrete-time voltages can be written as:

$$V_1(k+1) = V_1(k) - \frac{T_s \times S_b}{C_1} i_{inv}(k) \tag{3.30}$$

$$V_2(k+1) = V_2(k) - \frac{T_s \times S_c}{C_2} i_{inv}(k) \tag{3.31}$$

3.9 Conclusion

This chapter covers the design of active power filter using both conventional and PEC9 inverters, along with the control techniques MPC and FS-MPC respectively.

The next chapter will validate the effectiveness of the control design through simulation of the proposed system using MATLAB/SIMULINK.

CHAPTER 4

Simulation and Results

4.1 Introduction

This chapter evaluates the control performance and dynamic behavior of the proposed Multifunctional Solar Active Filter (Solar-AF) system based on the PEC9 inverter topology. The system is subjected to various perturbations to assess its robustness and adaptability under real-world operating conditions. The entire system, including control algorithms and power circuit components, was modeled and simulated using MATLAB/Simulink. The results aim to validate the effectiveness of the Solar-AF system in performing multiple functions, such as active power injection, harmonic compensation, and reactive power support, under varying environmental and load scenarios.

4.2 PEC9 Solar-AF Using MATLAB Environment

Figure 4.1 describes the general circuit of the system, it represents the proposed Solar-AF which is arranged in parallel with a nonlinear load and the grid supply. The system consists of the PV array of 36 modules and delivering up to 150 Watts(under STC) where it is constructed of 4 modules in series and 9 in parallel. The maximum power is extracted across the boost converter at voltage of18.65 V and at current of 8.04 A. classical inverter then using the 9-level PEC inverter, and it is also the interconnection between the system and the grid utility.

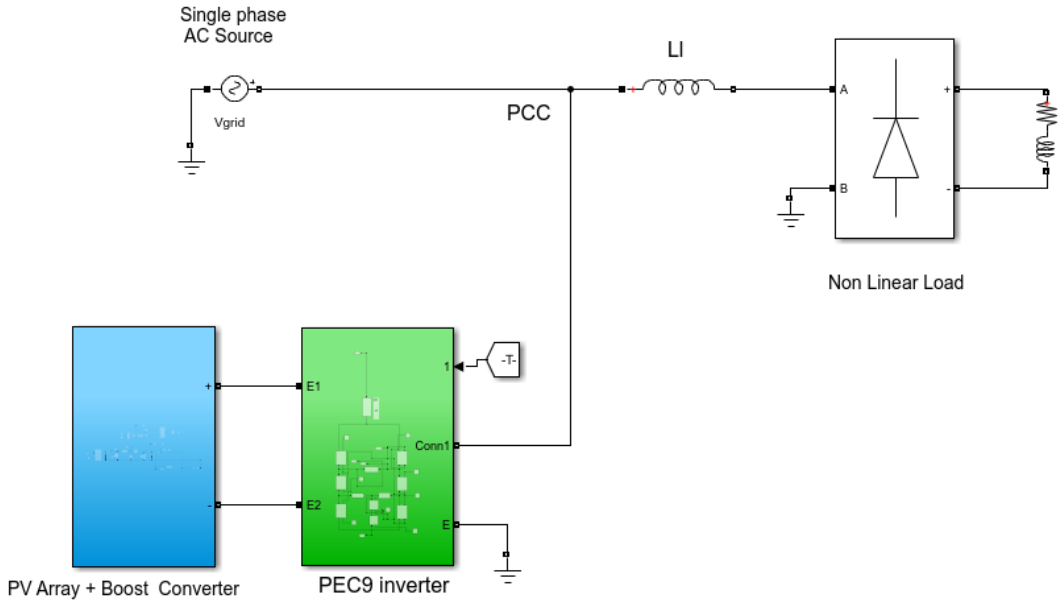

Figure 4.1: General scheme of the system

4.3 PEC9 Solar-AF Parameters

The values of the used components, elements and other parameters are indicated in the table below (Table 4.1).

Table 4.1: The general parameters values of the Sola-AF.

Grid	Phase to phase RMS Voltage	63 V
	Frequency	50 Hz
	DC voltages (V_1&V_2)	(150/4) V
	DC voltage reference (V_{dc}*)	150V
PV generator	Maximum power (STC)	150W
	Voltage at MPP	18.65 V
	Current at MPP	8.04A
	DC-LinK Capacitance (C_1&C_2&C_3)	2500 μF
	Short-circuit current I_{sc}	8.49A
	Open circuit voltage V_{oc}	22.64V
Boost converter	Capacitor	47μF
	DC-link Capacitor	390 μF
	DC-link voltage	150 V
Filter side inductor	L_f	15 mH
Load side inductor	L_i	5 mH
Load side resistance	(R_L)	100 Ω
Load side inductance	(L_L)	0.7 mH
Additional load resistance	(R_L)	29 Ω

The I-V and P-V characteristics corresponding to the used (user-defined) PV module are shown in Figure 4.2.

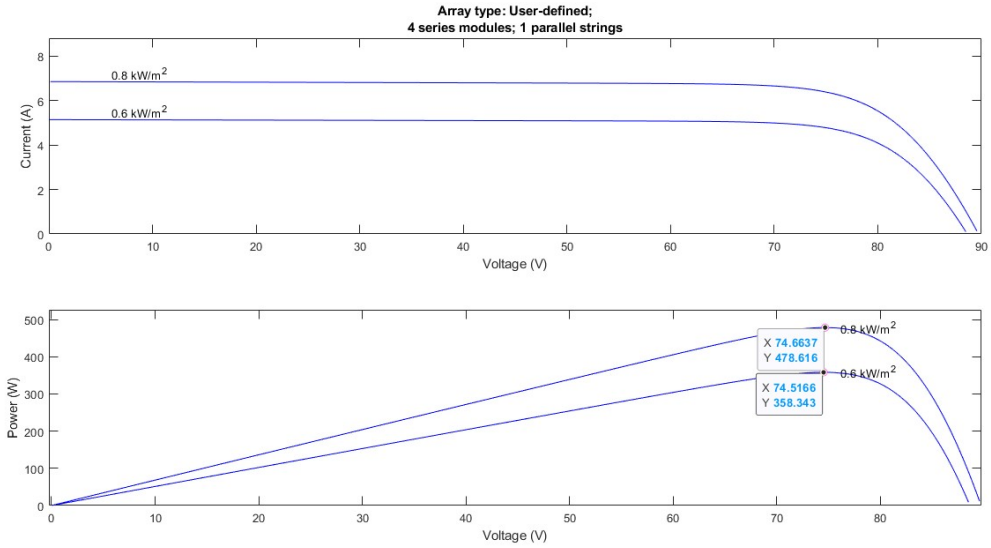

Figure 4.2: The I-V and P-V characteristics of the used PV module (under STC)

4.4 Shunt-APF With Single Phase Conventional Inverter using MATLAB Environment

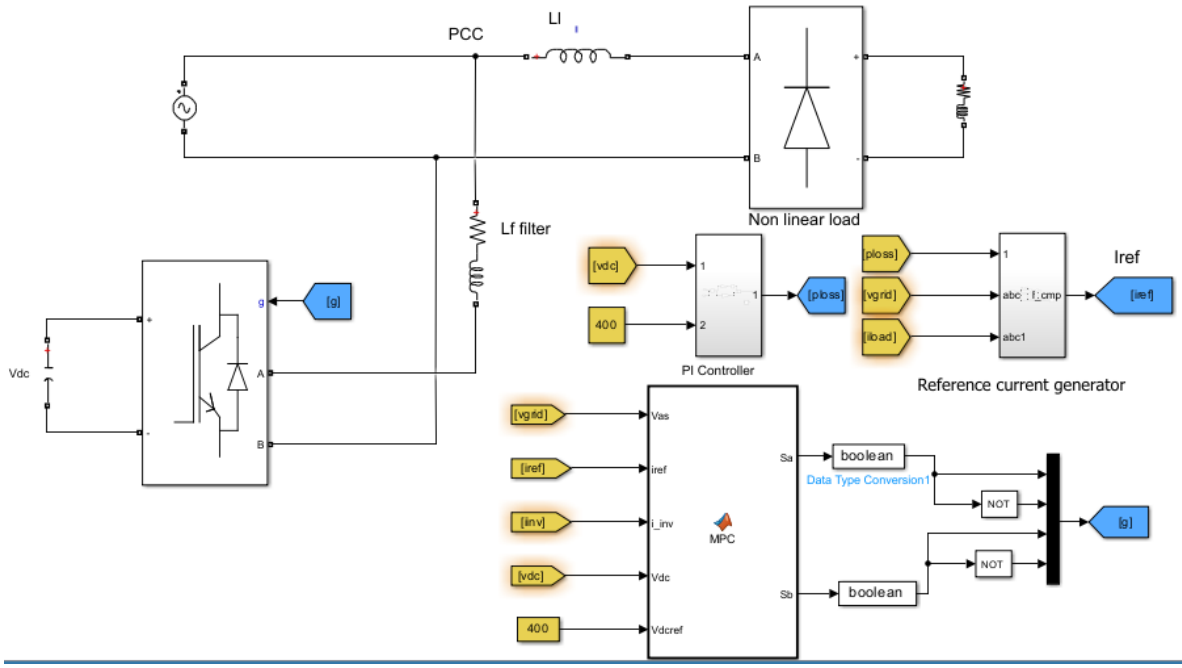

Figure 4.3: The simulated system of classical two level inverter

4.5 Conventional Active Filter Parameters

The values of the used components for the conventional simulated inverter are shown in the table below.

Table 4.2: Shunt-APF SIMULATION SYSTEM PARAMETERS

AC grid voltage	63 (RMS)
AC grid frequency	50Hz
Filter side inductor (L_f)	20mH
Filter side resistor (R_f)	2.5mΩ
Load side inductor (L_i)	5mH
DC voltage reference (V_{dc}*)	150V
DC-Link capacitor Capacitance (C)	1500μF
Load side resistance (R_L)	30Ω
Load side inductance (L_L)	3H
Switching frequency (f_s)	40KHz

4.6 Simulation Results

The results of DC link voltage , source current, load current, and the inverter current ar shown below.

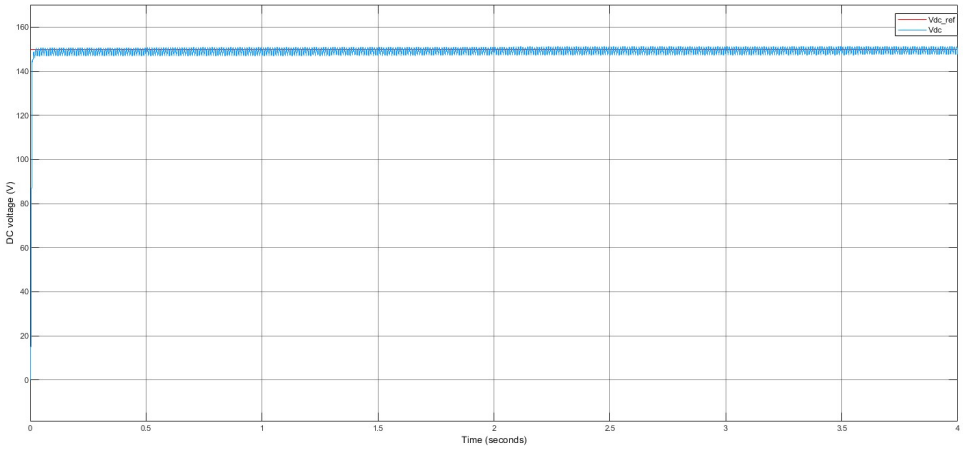

Figure 4.4: DC link voltage

The load current is noticeably distorted due to the nonlinear nature of the connected load as shown in figure 4.5, exhibiting significant harmonic components. This waveform is non-sinusoidal, confirming the need for harmonic compensation through the SAPF. The Total Harmonic Distortion (THD) of the load current is relatively high, reflecting poor power quality prior to compensation.

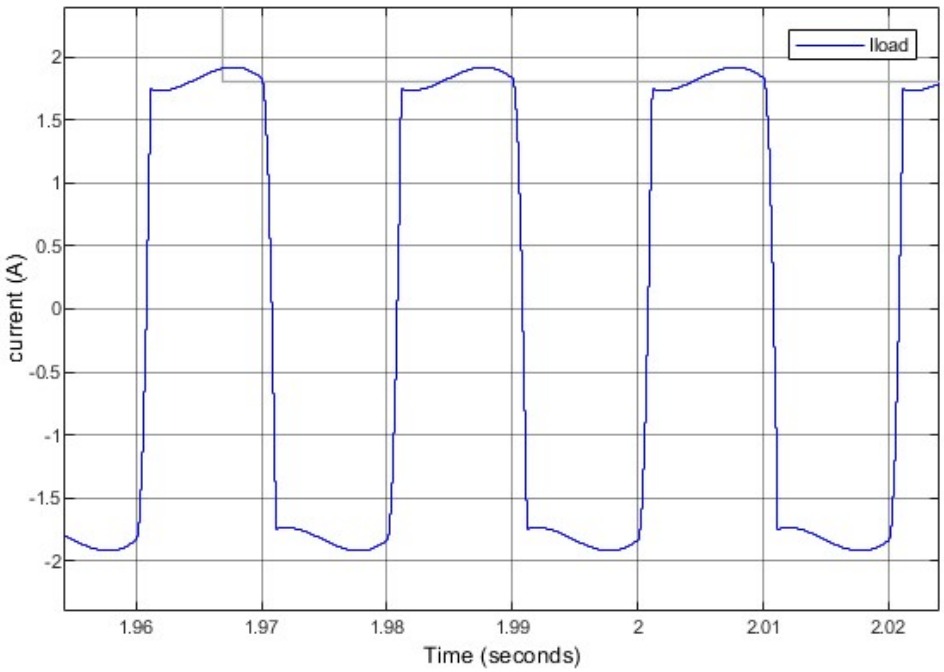

Figure 4.5: load current

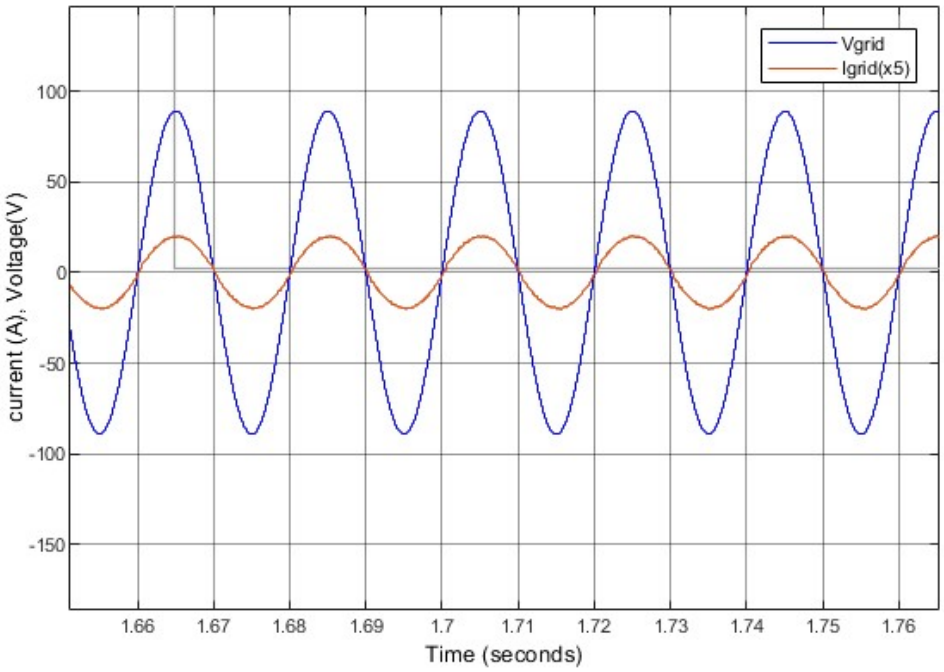

Figure 4.6: Grid current and voltage

After compensation, the grid current becomes nearly sinusoidal, indicating effective harmonic mitigation by the SAPF. The Total Harmonic Distortion (THD) of the source current is significantly reduced, typically meeting the IEEE 519 standard ($< 5\%$). This demonstrates that the active filter successfully isolates the grid from the nonlinear effects of the load.

For the current injected by the inverter as shown in figure 4.7, The waveform is non-sinusoidal, as expected, since it is designed to inject only the harmonic components. The dynamic response of the inverter shows good tracking of the reference during steady-state and transient conditions.

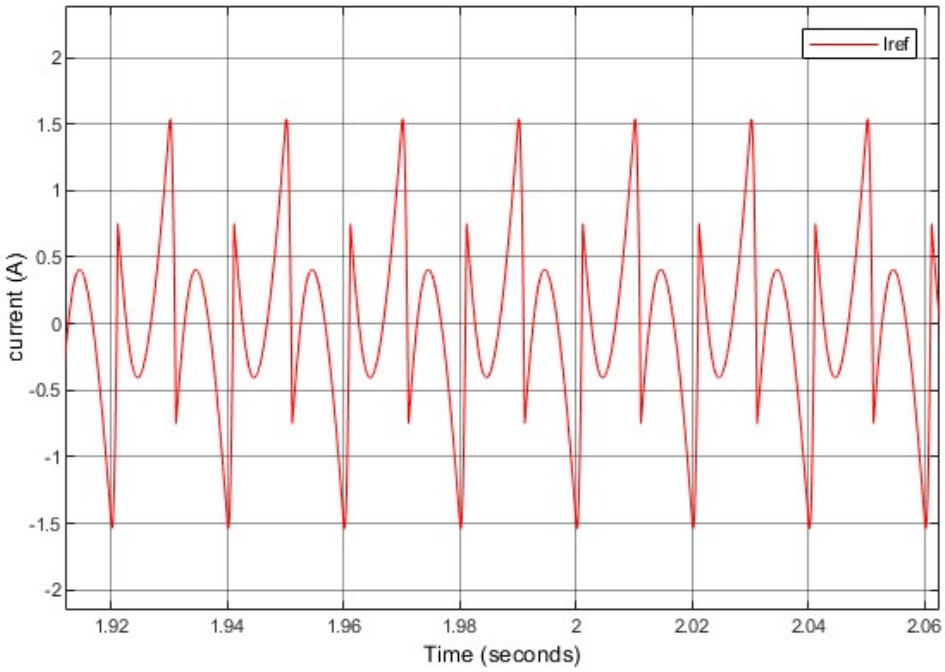

Figure 4.7: Reference current

As far as the harmonic content is concerned, a fast Fourier transform (FFT) analysis of signals is performed as well as showing the THD value of the grid current.As it is shown, the THD is 4.15% (Figure 4.6) which is relatively low (less than 5% according to IEEE 519).

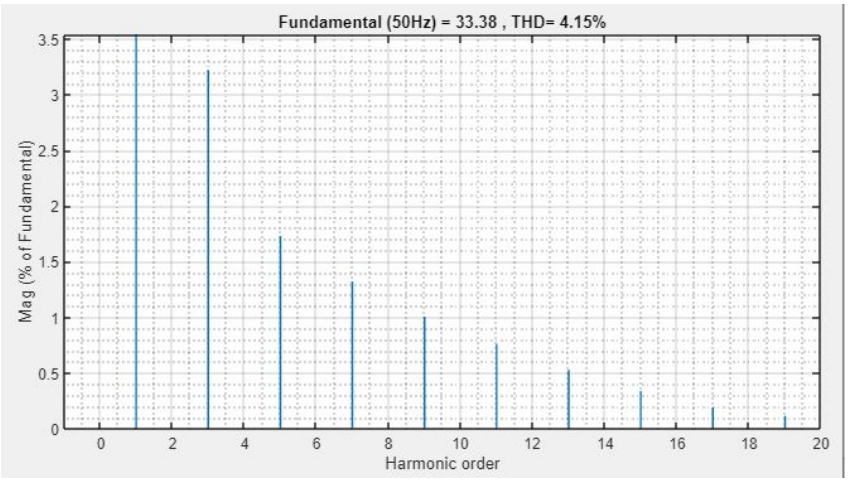

Figure 4.8: FFT analysis tool for the grid current

4.7 Grid Connected PEC9 Inverter Using MATLAB Environment

The Grid connected PEC9 inverter system depicted in Figure 4.9 was modeled in MATLAB/Simulink to evaluate its ability. The inverter is controlled using a Finite Set Model Predictive Control (FS-MPC) algorithm, which selects the optimal switching state based on current and voltage predictions. The control strategy ensures proper tracking of the reference current and maintains balanced capacitor voltages.

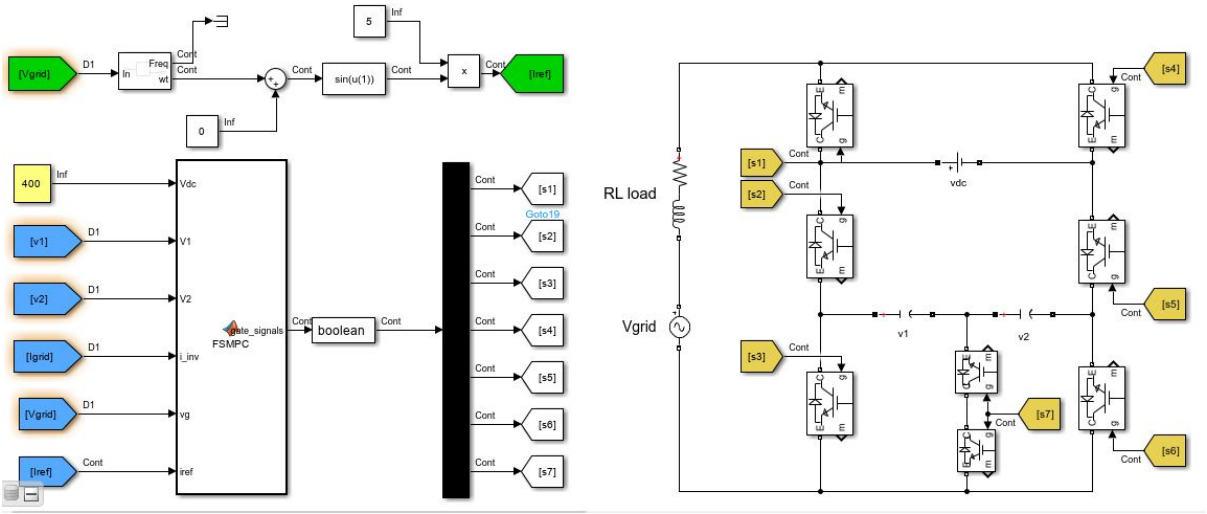

Figure 4.9: The Simulated System of Stand Alone PEC9 inverter

4.7.1 Grid Connected PEC9 Parameters

The values of the used components for the stand alone simulated inverter are shown in the table below.

Table 4.3: Grid connected PEC9 system parameters

AC source voltage	63 (RMS)
Fundamental frequency	50Hz
Grid filter inductor (L_f)	15mH
Grid filter resistor (R_f)	2mΩ
DC voltage reference (V_{dc}*)	150V
DC-Link capacitors Capacitance (C_1&C_2)	2500μF(for each)
Switching frequency (f_s)	30KHz

4.8 Simulation Results

The following figures illustrate the simulation waveforms obtained from the MATLAB/Simulink model. Figure 4.10 shows the source voltage and current, the source current exhibits a sinusoidal shape with minimal distortion, demonstrating the inverter's ability to supply a clean current waveform. This confirms that the FS-MPC effectively regulates the inverter switches to synthesize a current that accurately follows the reference.

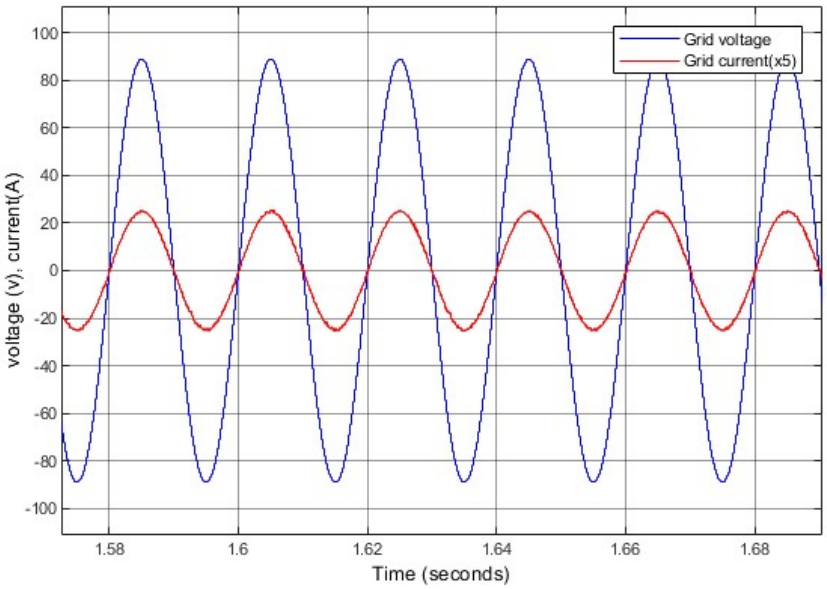

Figure 4.10: Grid current and voltage

As observed in the FFT analysis Figure 4.11, the THD of the source current is maintained within acceptable limits 1.94% (according to IEEE 519 standards), confirming that the inverter injects a clean current into the load.

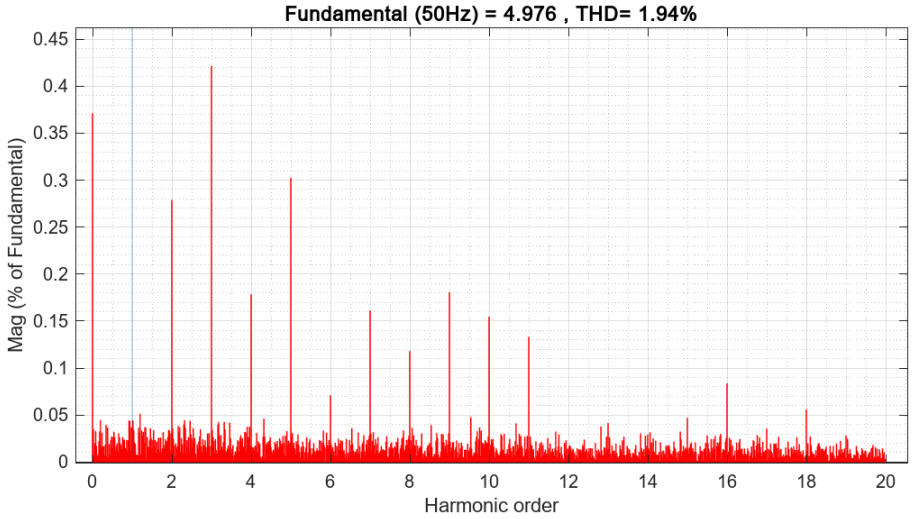

Figure 4.11: FFT analysis for the source current

The inverter output shows a nine-level voltage waveform, which confirms the proper operation of the PEC9 topology as it appears in figure 4.12 nine levels are clearly produced.

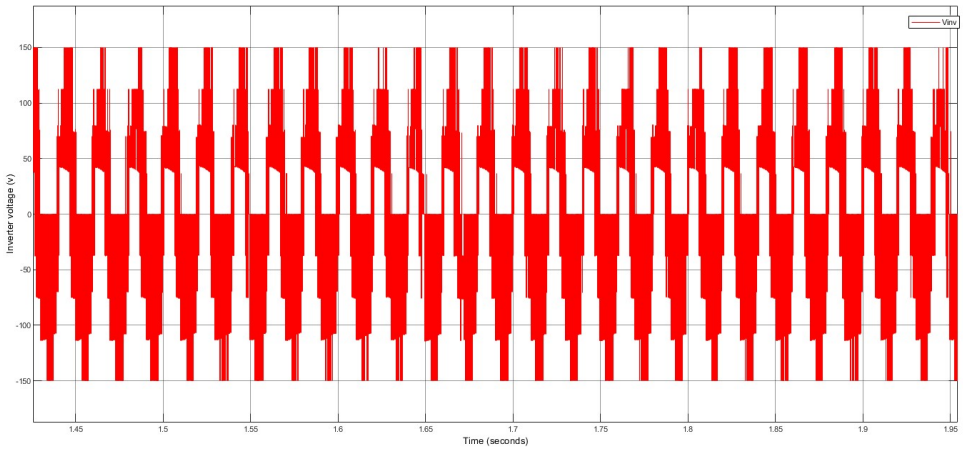

Figure 4.12: PEC9 inverter voltage

Then, the capacitor voltages V1 and V2 remain well-balanced around their desired values throughout the operation.

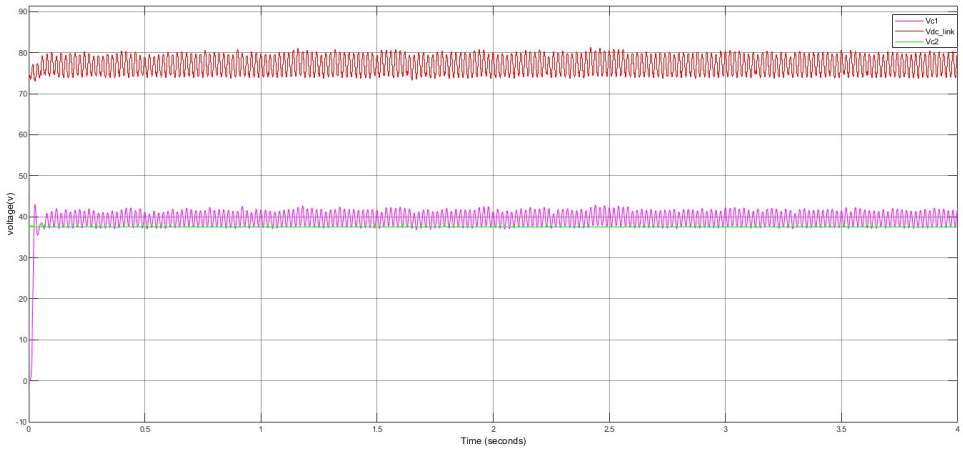

Figure 4.13: DC link capacitors voltage

A slight increase in the voltage of capacitor V1 was observed during the simulation. This small deviation may be attributed to the asymmetric operation of the switching states or dynamic changes in the load. However, the variation remains within acceptable limits and does not affect the overall performance or output voltage levels. The control strategy effectively maintains voltage stability and ensures reliable performance of the inverter.

4.9 PEC9 Single-phase inverter-based Solar-AF

In this section, the single-phase PEC9 inverter is compared in terms of component count, switching frequency, voltage rating, and Total Harmonic Distortion (THD).

The single-phase PEC9 inverter system consists of a single-phase PEC9 unit, which is a multilevel inverter capable of generating nine output voltage levels. This inverter is composed of a single isolated DC source , seven active switches (this would include 6 bidirectional switches and a single four-quadrant switch), along with two DC capacitors that are actively balanced. This design aims to significantly reduce the number of components compared to conventional single-phase inverters that might use more switches or multiple DC sources to achieve similar voltage levels, leading to an improvement in Total Harmonic Distortion (THD) and system efficiency.

The inverter unit is fed by a PV array that generates a rated power of 150 W, extracted at a voltage of 18.65 V and a current of 8.04 A (STC). This array is constructed of 4 modules connected in series and 1 modules connected in parallel.

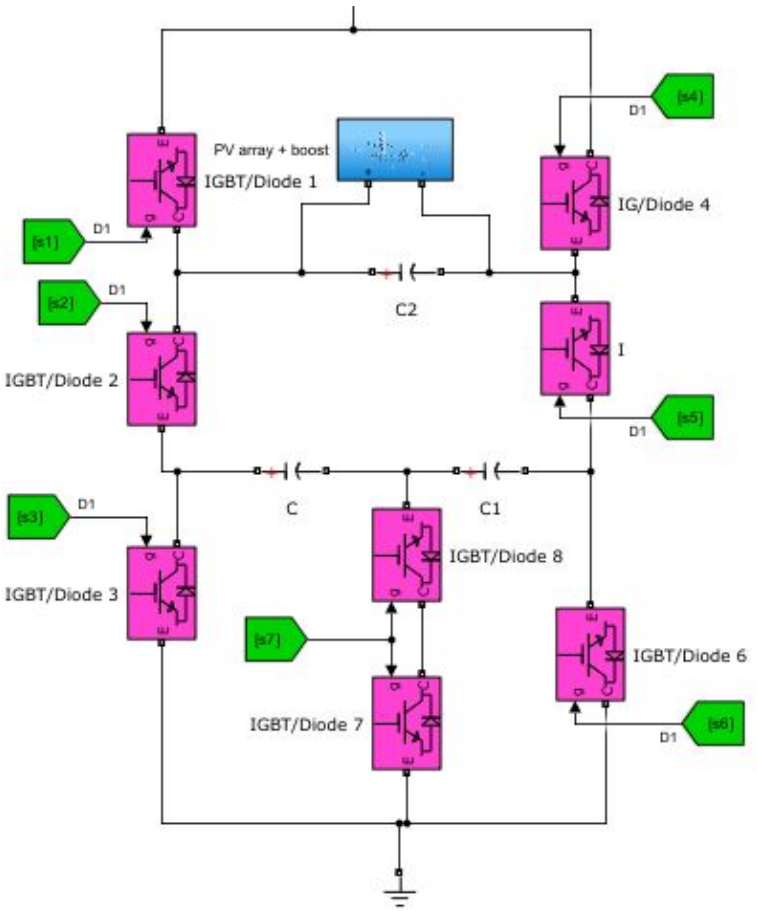

Figure 4.14: the simulated system of the single phase PEC9 inverter-based Solar-AF

4.10 Simulation Results

The results of PV output voltage (Vpv), current (Ipv) are shown in figure 4.16 ,where the power (Ppv) , DC link voltage (Vdc) are shown in figure 4.17 under diffrent irradiance scenarios (1000 W/m2, 600W/m2,and 800W/m2)

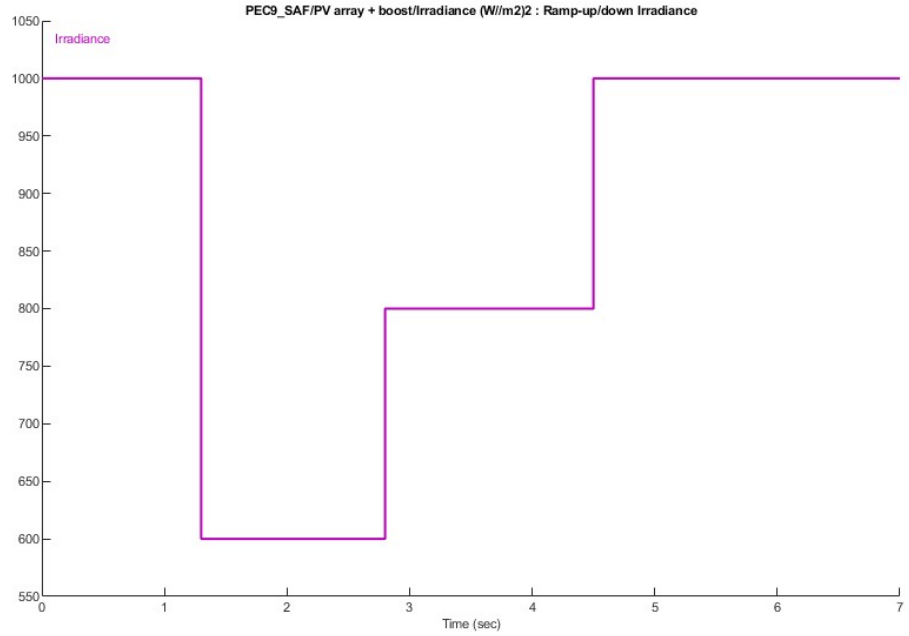

Figure 4.15: Irradiance profile of the simulated system

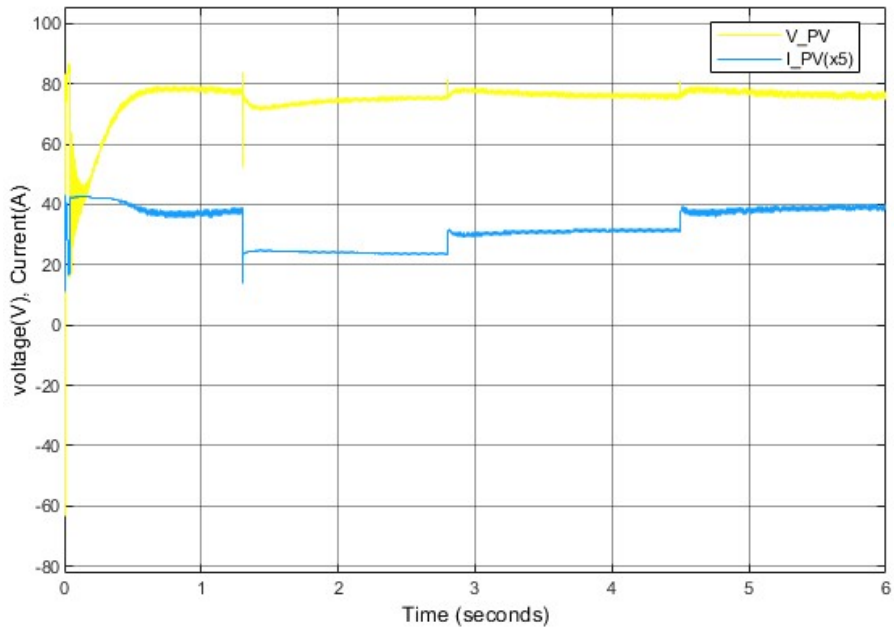

Figure 4.16: Demonstration PV Output Voltage and Current, under different irradiance scenarios

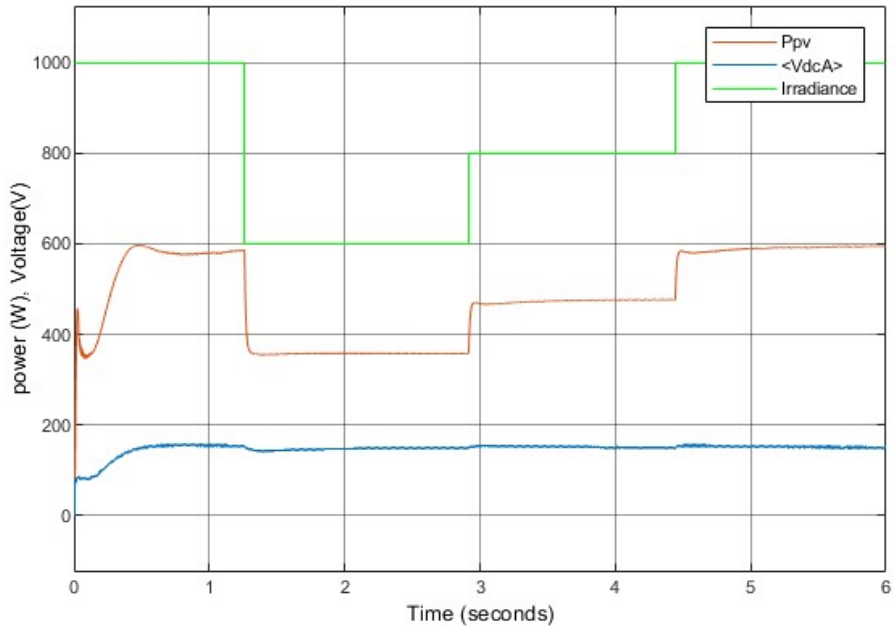

Figure 4.17: Demonstration PV Output power and boost converter under different irradiance scenarios

Figure 4.18 illustrates the power distribution between the photovoltaic (PV) system (Ppv), the load (Pload), and the utility grid (Pgrid) under a solar irradiance levels of 600 W/m² and 800 W/m² and 1000 W/m². The plots demonstrates the system's dynamic response and stable operation, highlighting effective energy management between generation,consumption, and export.

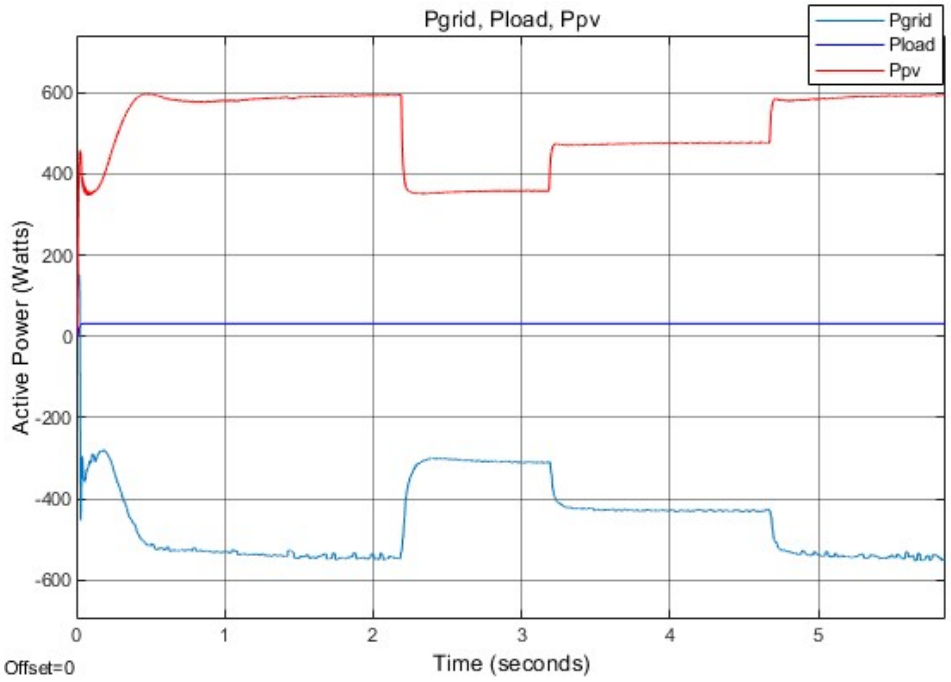

Figure 4.18: Active power curves of source, load and inverter during the simulation time using PEC9 inverter at 600 W/m², 800 W/m², and 1000 W/m²

The high accuracy of active and reactive power compensation is obvious on its curves. Initially, the system exhibits a high level of reactive power due to the nonlinearity of the load. However, once the PEC9 inverter is activated and synchronized with the grid, the reactive power rapidly drops and stabilizes near zero and unity power factor is achievable

.

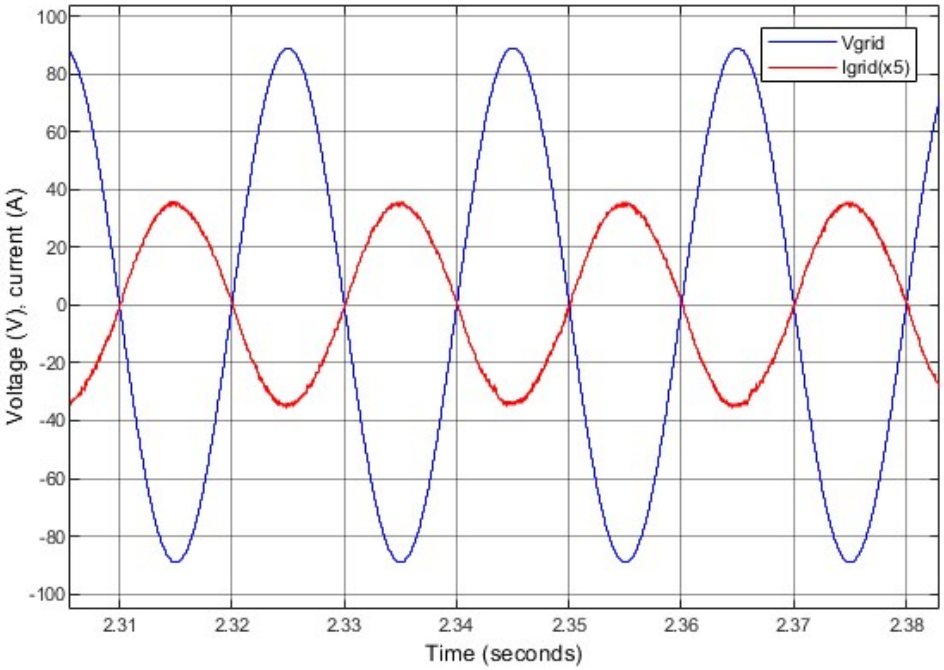

Figure 4.19: Grid voltage and current(x5)

The simulation results in figure 4.20 shows that the DC-link voltage (Vdc) is well-regulated, providing a stable power supply to the PEC9 inverter. The capacitor voltages, V1 and V2, are effectively balanced around their target values even at different scenarios, enabling accurate nine-level voltage generation.

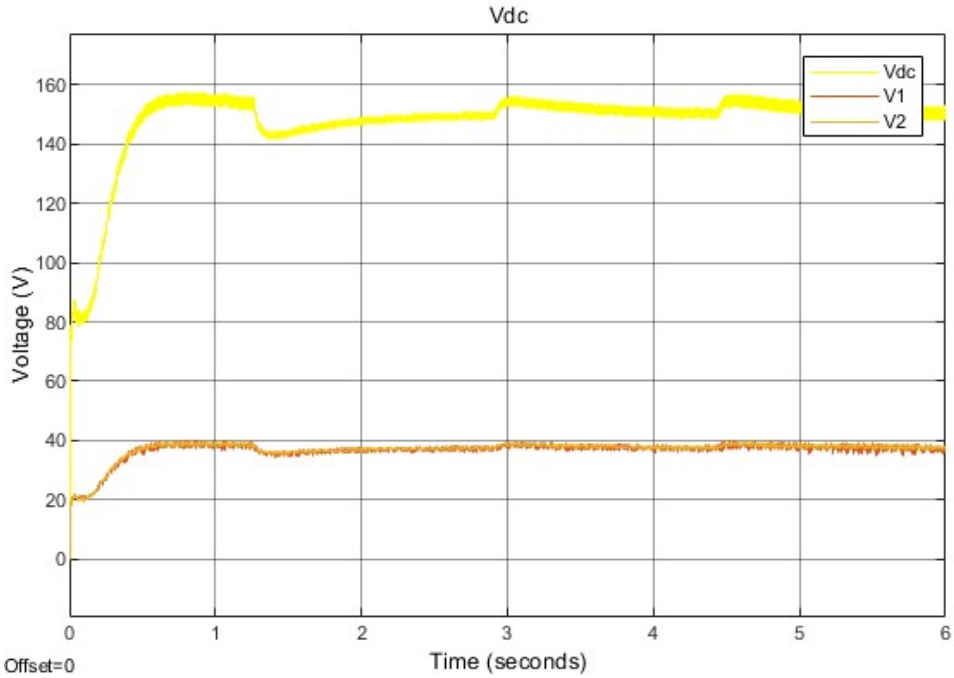

Figure 4.20: DC link Capacitors Voltages

V1 and V2 are set to one fourth of Vdc . which allows generating a perfect nine level(± Vdc/4, ±Vdc/2, ±3Vdc/4, ±Vdc and 0) as depicted in figure 4.20.

The inverter output voltage (Vinv) depicted in figure 4.21 clearly demonstrates the expected multilevel waveform, confirming correct switching operation, efficient voltage balancing, and high-quality power injection into the grid. The output phase voltage is 9-level (± 150v ,±112.5,±75,±37,5 and 0).

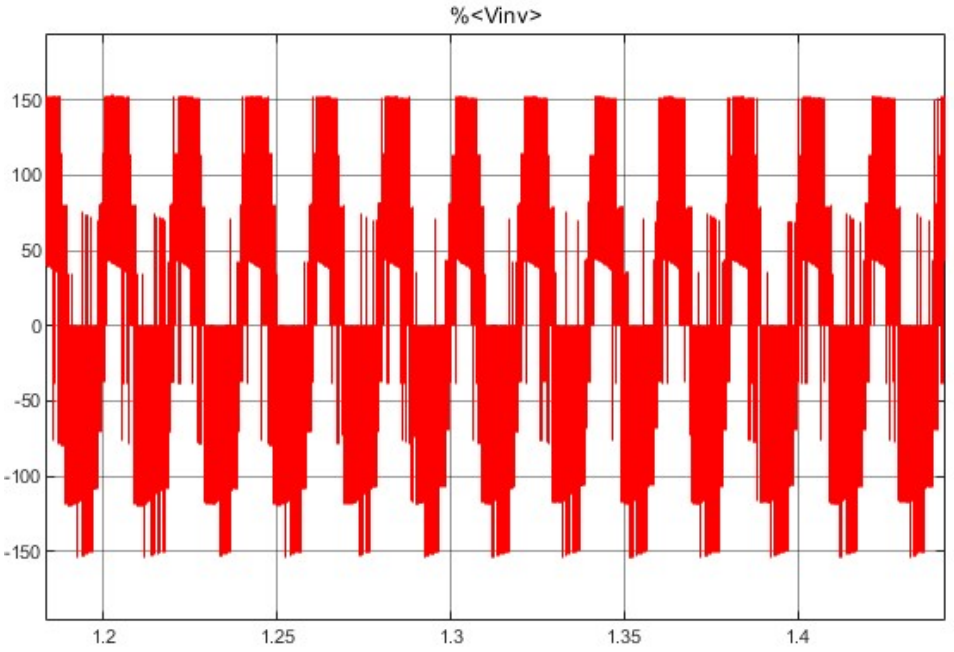

Figure 4.21: PEC9 output voltage

To validate the above analysis, a focused evaluation was carried out on key parts of the simulation, particularly the current waveforms and the FFT analysis of the source current, with special attention given to the Total Harmonic Distortion (THD).

4.10.1 System performance at irradiance of 600 W/m², 800 W/m², and 1000 W/m²

Figure 4.23 makes it evident that the suggested controller can extract the MPP from each PV array by maintaining the array's irradiance at 600 W/m², 800 W/m², and 1000 W/m²(STC) constant. Also, the inverter-generated current that also includes compensating harmonic components (power injection mode and harmonic mitigation). A pure sinusoidal current is thus being absorbed by the source.

Figure 4.22 clearly shows the changing of load , grid, and inverter current under different scenarios of irradiance.

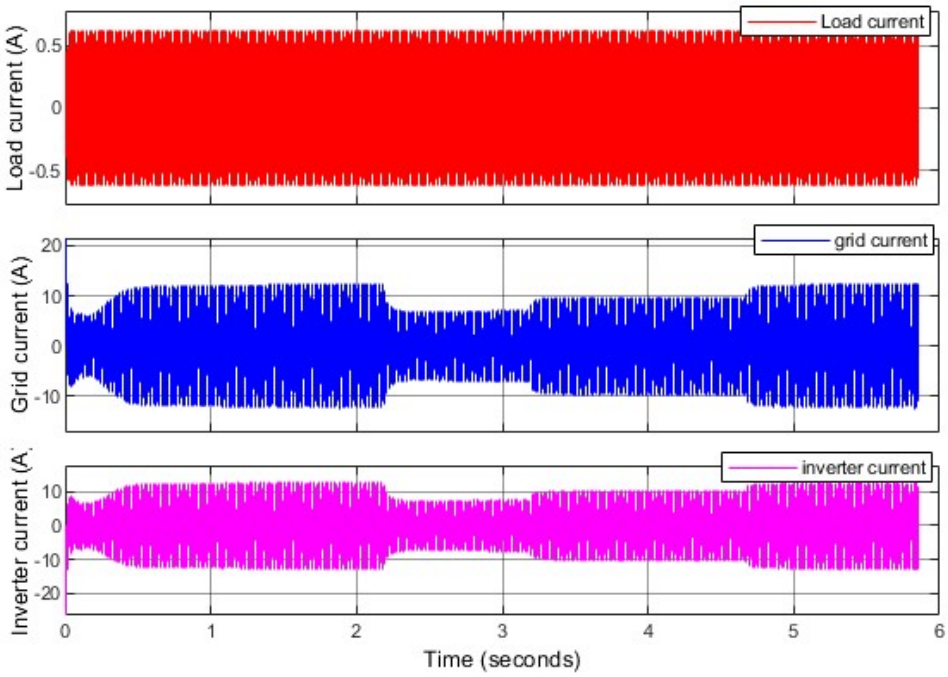

Figure 4.22: demonstration of grid current, load current and filter current under 600 W/m², 800 W/m², and 1000 W/m²

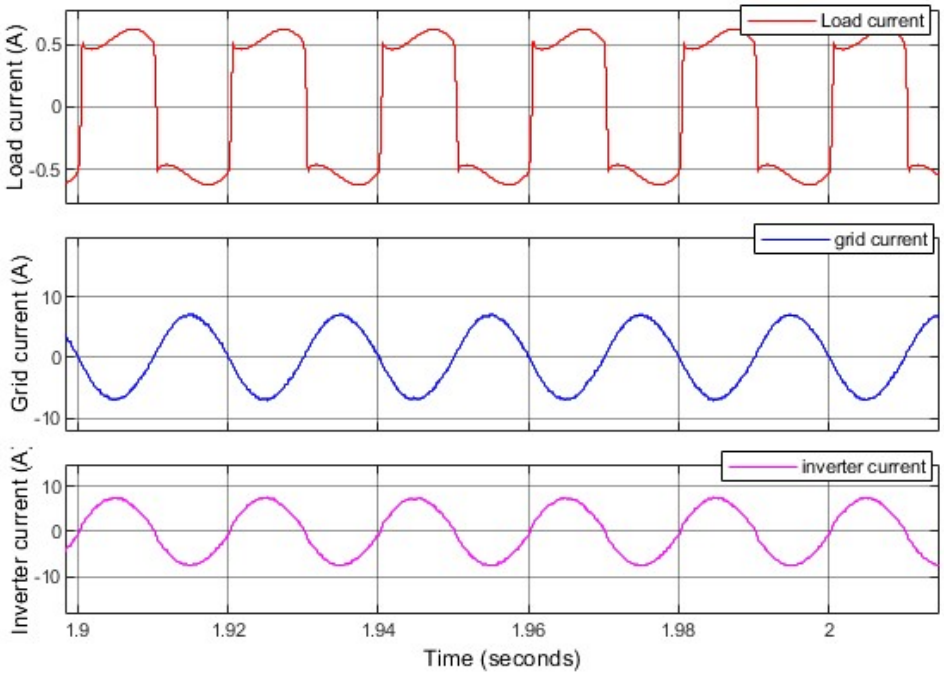

Figure 4.23: Demonstration of grid current, load current and filter current under 600 W/m²

Figure 4.25 shows the THD measurement of current 2.85% that is a good result under irradiance 600 W/m² which is less than 5% according to IEEE 519-1992.

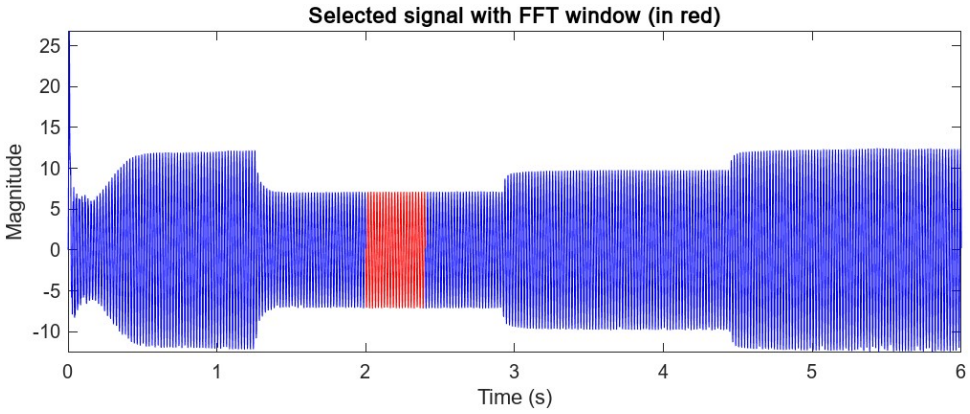

Figure 4.24: FFT window under 600 W/m2

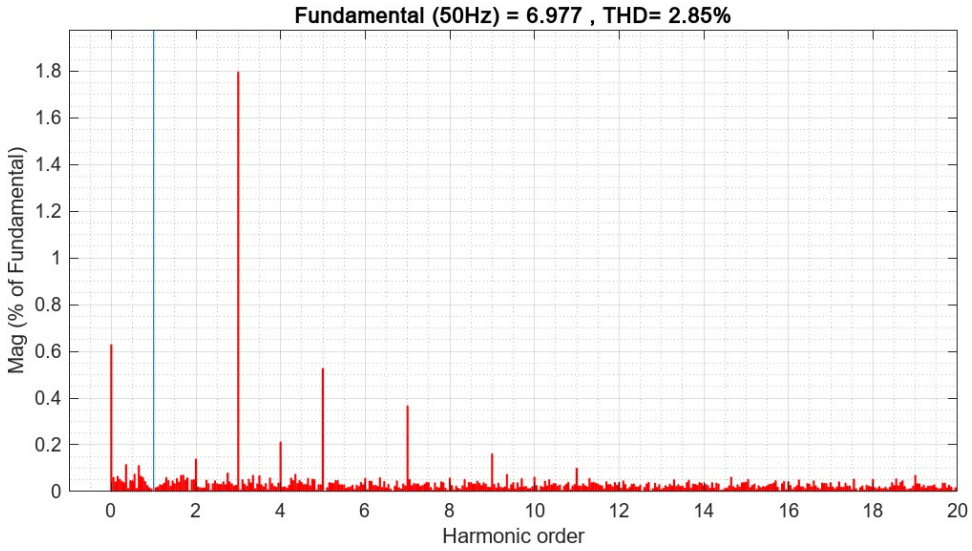

Figure 4.25: FFT analysis tool for the source current of the system under 600 W/m2

Figure 4.28 shows the THD measurement of current 2.7% that is a good result under irradiance 800 W/m^2 which is less than 5% according to IEEE 519-1992.

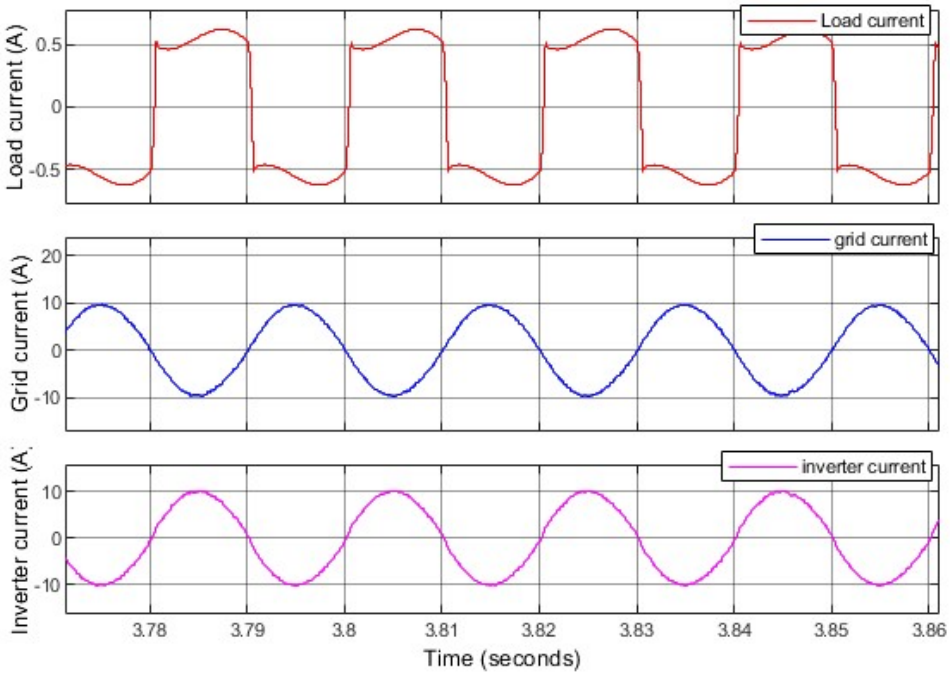

Figure 4.26: Demonstration of grid current, load current and filter current under 800 W/m^2

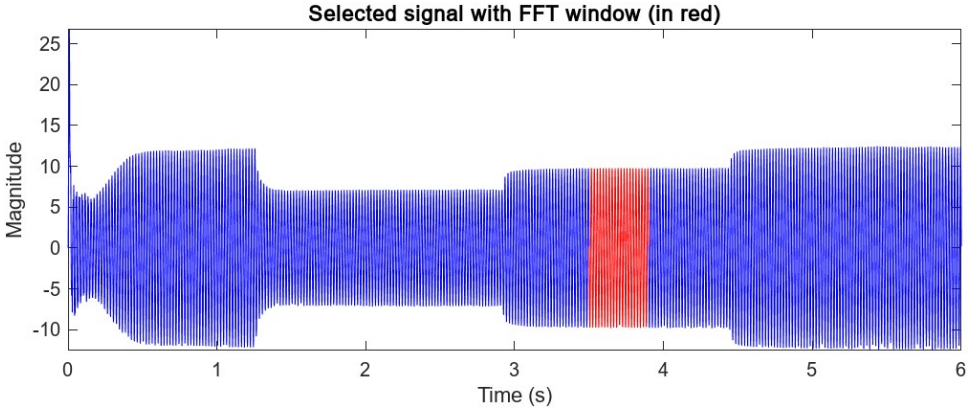

Figure 4.27: FFT window under 800 W/m2

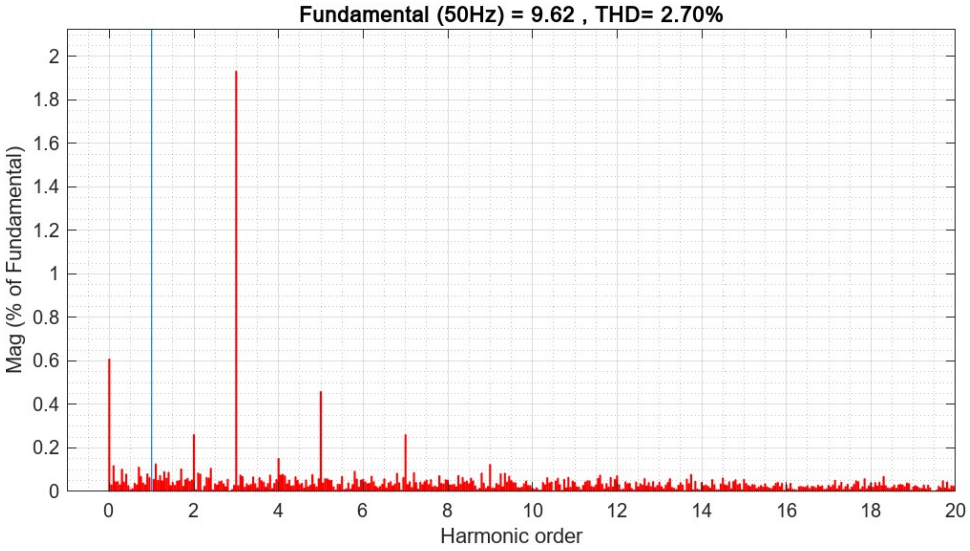

Figure 4.28: FFT analysis tool for the source current of the system under 800 W/m^2

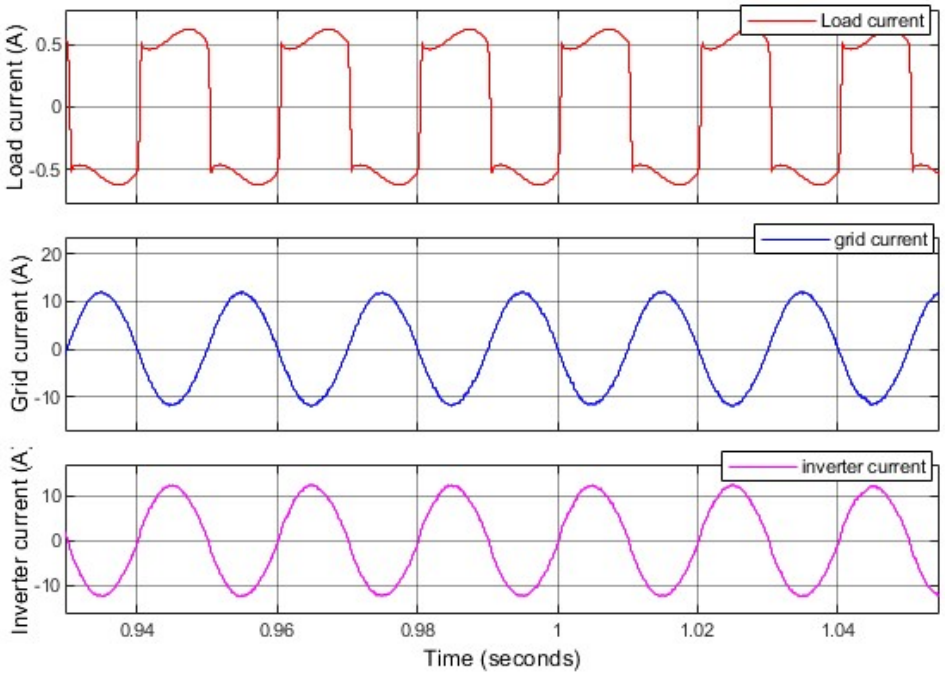

Figure 4.29: Demonstration of grid current, load current and filter current under 1000 W/m²

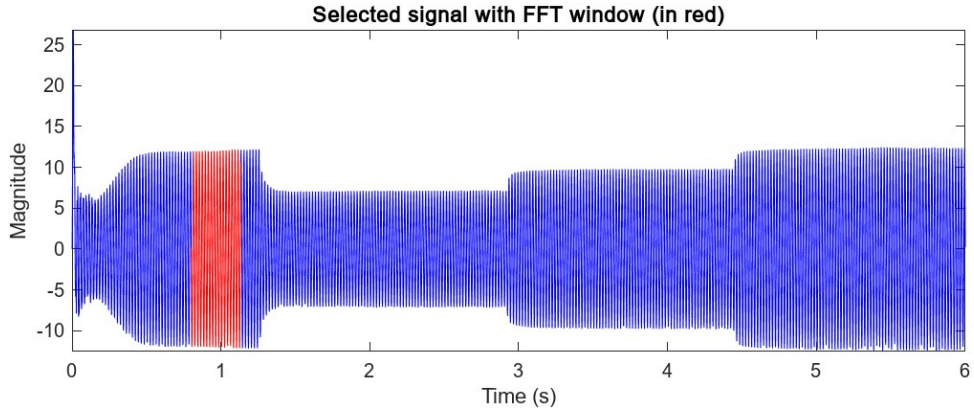

Figure 4.30: FFT window under 1000 W/m2

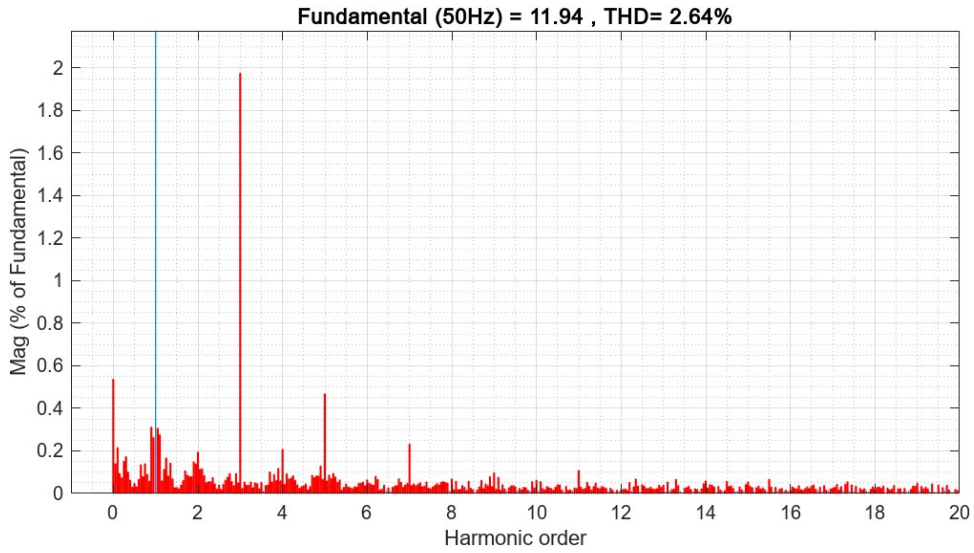

Figure 4.31: FFT analysis tool for the source current of the system under 1000 W/m²

Figure 4.31 shows the THD measurement of current 2.64% that is a good result under irradiance 1000 W/m² which is less than 5% according to IEEE 519-1992.

4.10.2 System Performance at Irradiance 800 W/m² With Additional Load Demand

The system is working under irradiance condition of 800 W/m² but with extra load demand (Parallel load), the current shape is so identical to be seen with the eye, however The THD is slightly increased with a value of 4.39% but it still within the acceptable range less than 5% according to IEEE 519-1992.

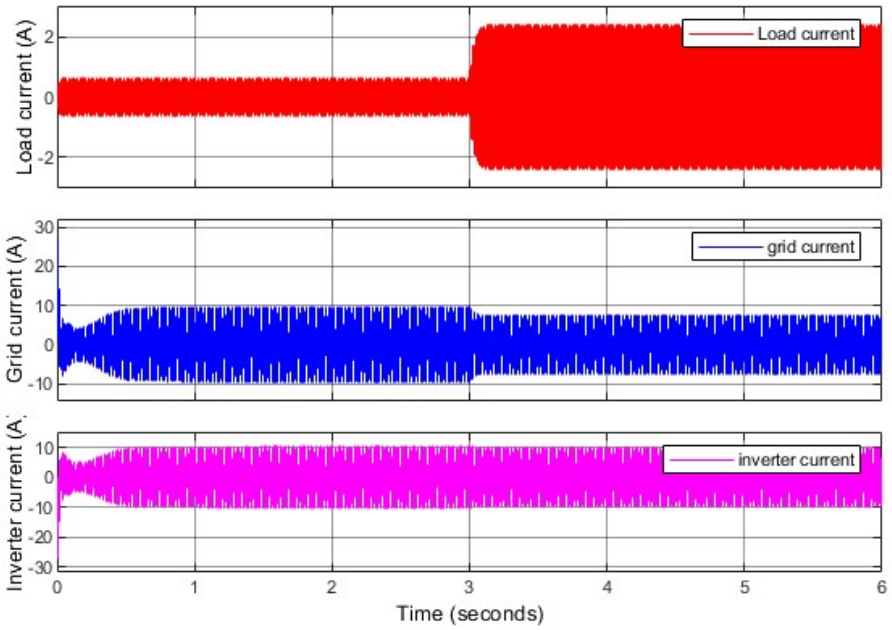

Figure 4.32: Demonstration of the grid current, Load current, and filter current under extra load demand

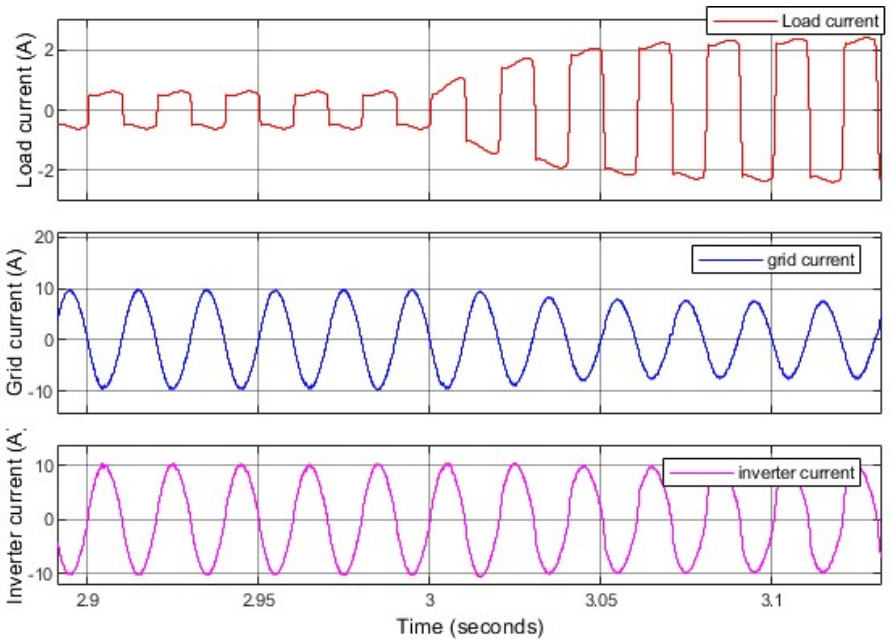

Figure 4.33: Demonstration of the changing of the grid current, Load current, and filter current under additional load demand

Even we have added extra load, the system still behaves optimally. The voltage of the two capacitors is balanced at the reference values as we can see in figure 4.34, and the the power balance equation is satisfied highlighting effective energy management between generation,consumption, and export as figure 4.35 shows.

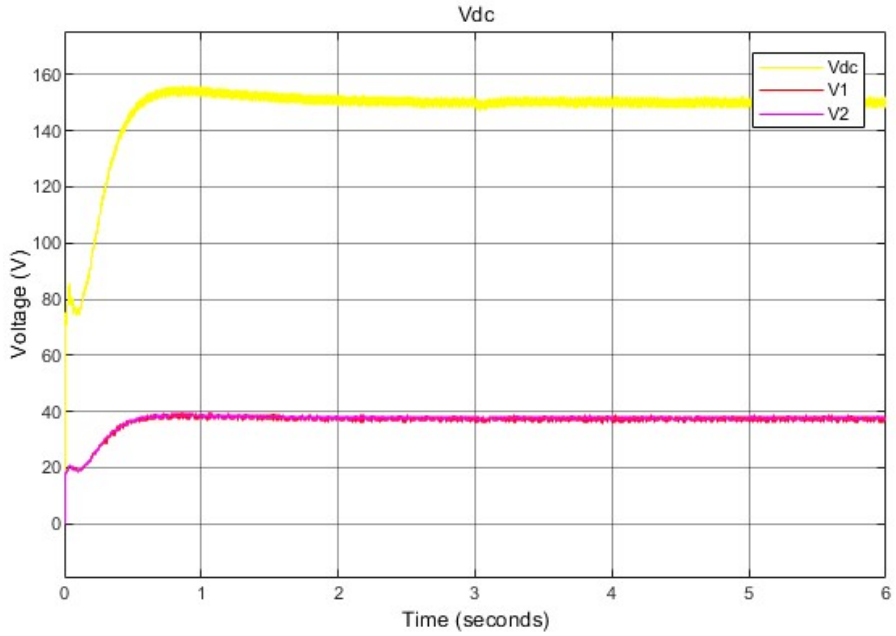

Figure 4.34: DC link capacitors voltage under additional load demand

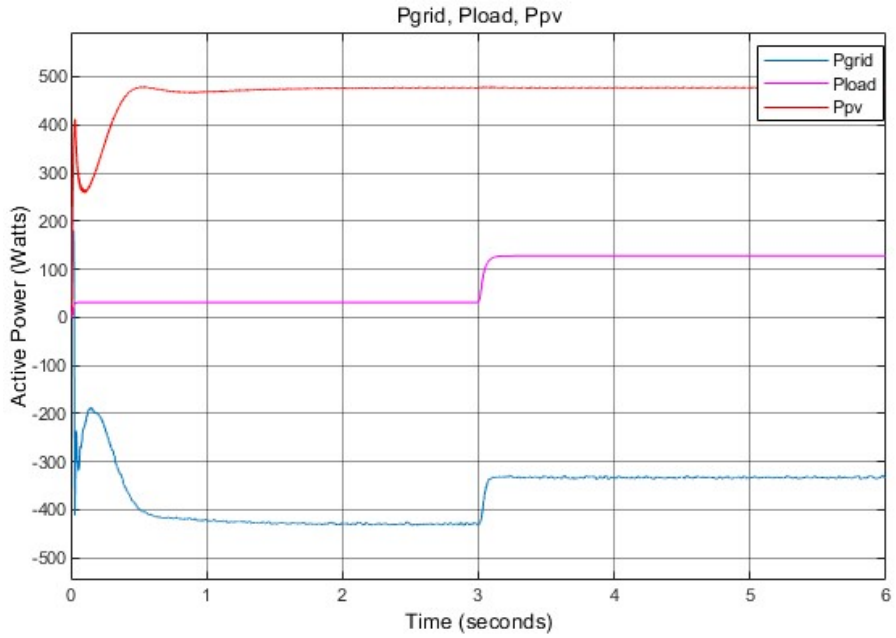

Figure 4.35: Active power curve of the PV, grid, and load under additional load demand

as we can see in figure 4.35 the load demand increased at 3s hence the grid power decreased. the resulting THD is depicted in figure 4.36.

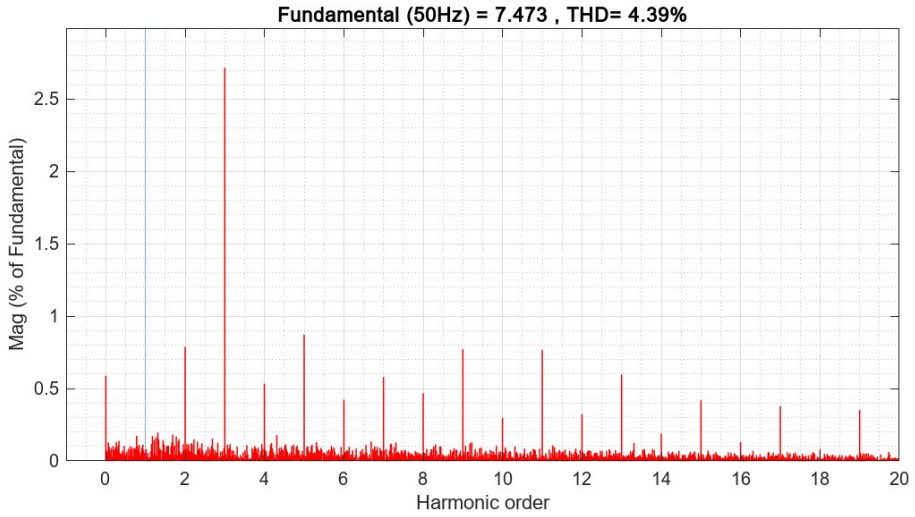

Figure 4.36: FFT analysis tool for the source current of the system under additional load demand

4.11 System Evaluation

The purpose of the evaluation is to compare the system's simulation results in terms of THD, and power losses when using the PEC9 inverter versus the classical inverter.

It is evident that PEC9 with a THD= 2.85% at irradiance 600 W/m2, a THD= 2.7% at irradiance 800 W/m2 , and a THD= 2.64% at irradiance 1000 W/m2 outperformed the Classical inverter with a THD= 4.15% . the same thing for the grid connected that proves its performance by achieving a THD= 1.94%. Thus, providing more proof that the THD is reduced by adding additional levels to the voltage waveform.

4.11.1 Results Discussion

- Based on the active power curves shown in Figures 4.18 , we can conclude that the suggested system can operate in either power injection mode or shunt AF mode, contingent on available irradiance, load demand, and harmonic distortions.

- The suggested Solar-AF system can extract peak power from a photovoltaic (PV) array, and guarantee a unity power without being affected by the irradiance deviations, and also eliminate harmonic currents, reactive power compensation, grid current balancing, and adaptive DC link voltage regulation.

- Because it produces more voltage levels at the output than a traditional grid-

connected inverter, significantly reducing the harmonic content of the injected current and achieving a low Total Harmonic Distortion (THD).This confirms the inverter's effectiveness in producing a clean current waveform suitable for grid integration. Moreover, the proposed design uses fewer switching devices, capacitors, and a smaller L filter than other multilevel topologies, which simplifies the system and enhances overall efficiency. Reducing the number of power components not only lowers the cost and complexity but also minimizes switching losses, which tend to increase with more components. These results validate the PEC9 inverter as a compact, efficient, and high-performance solution for grid-connected solar active filtering applications.

- The simulation results robustly validate the efficacy and superior performance of the proposed PEC9-based SAPF system. Notably, the system consistently achieved significant harmonic mitigation, evidenced by Total Harmonic Distortion (THD) values of the grid current well below the stringent IEEE 519 standard's 5% limit. Specifically, THD values as low as 2.85% at 600 W/m^2, 2.7% at 800 W/m^2, and 2.64% at 1000 W/m^2 were demonstrated, significantly outperforming a conventional two-level inverter (which yielded a 4.15% THD). This remarkable reduction in harmonic content is a direct consequence of the PEC9 inverter's ability to synthesize a high-quality, nine-level output voltage waveform.

4.12 Conclusion

In summary, the PEC9-based solar active power filter effectively combines power quality improvement and renewable energy integration. With reduced harmonic distortion less than 5%, balanced capacitor voltages, unity power factor, and fewer components than conventional multilevel inverters, the system proves to be both efficient and reliable for grid-connection and active filtering applications.

GENERAL CONCLUSION AND FUTURE WORK

This thesis has presented the modeling, control, and simulation of a multifunctional solar active power filter based on the PEC9 multilevel inverter. The proposed system was developed to simultaneously inject photovoltaic (PV) power into the grid and enhance power quality by mitigating current harmonics and compensating reactive power drawn by nonlinear loads.

The system integrates a photovoltaic generator, a boost converter using the Perturb and Observe (P&O) algorithm for maximum power point tracking (MPPT), and a PEC9 multilevel inverter controlled via Finite Set Model Predictive Control (FS-MPC). The modified PQ theory was employed for reference current generation, enabling the inverter to deliver the exact compensating currents required to achieve a sinusoidal grid current and unity power factor.

The PEC9 topology, known for its reduced number of switches and passive components, proved effective in generating a high-quality nine-level output voltage, which significantly reduced the Total Harmonic Distortion (THD) of the injected current. The simulation results confirmed the controller's ability to track the reference current accurately, maintain balanced capacitor voltages (V1 and V2), and ensure a stable DC-link voltage (Vdc).

The simulation results validate the system's ability to operate reliably in a grid-connected environment, and Active power filtering ensuring efficient energy transfer and enhanced power quality.

In conclusion, the developed PEC9-based solar active power filter successfully combines power generation and power quality improvement in a compact and efficient

configuration. It represents a promising solution for modern grid-connected PV systems, capable of meeting both energy delivery and power conditioning requirements.

4.13 Future Work

While the system achieved promising results, several enhancements can be explored in future work:

- **Optimization of Control Parameters:** The performance of the FS-MPC depends significantly on the selection of weighting coefficients. Future work can employ optimization techniques such as Particle Swarm Optimization (PSO) and Genetic Algorithms (GA) to automatically tune these coefficients and improve the controller's adaptability and accuracy under varying conditions.

- **Fault-Tolerant Operation:** Further investigation into the fault management of the PEC9 topology could enhance system reliability. Specifically, developing intelligent detection and control algorithms to smoothly transition the system between 9-level, 7-level, and 5-level operation during the bidirectional switch fault, and even produce more levels such as PEC13 topology would be a valuable improvement.

- **Experimental Validation:** Building a hardware prototype will be essential to validate the simulation results and address practical implementation challenges.

- **Extension to Three-Phase Systems:** The proposed control strategy and inverter topology can be extended to three-phase applications to suit industrial and commercial power systems with higher power demands.

BIBLIOGRAPHY

[1] f. b. O.ellabban, haitham abu-rub, "renewable enrgy resources : current status,future prospects and their enabling technology," *Elsevier*, pp. 748–764, 2014.

[2] F. Sebaaly, H. Y. Kanaan, J. Rodriguez, and K. Al-Haddad, "Direct predictive control for a nine-level packed e-cell (pec9) converter based shunt active power filter (sapf)," in *IECON 2021–47th Annual Conference of the IEEE Industrial Electronics Society*, pp. 1–7, IEEE, 2021.

[3] J. L. Afonso, M. Tanta, J. G. O. Pinto, L. F. Monteiro, L. Machado, T. J. Sousa, and V. Monteiro, "A review on power electronics technologies for power quality improvement," *Energies*, vol. 14, no. 24, p. 8585, 2021.

[4] M. Sharifzadeh and K. Al-Haddad, "Packed e-cell (pec) converter topology operation and experimental validation," *IEEE Access*, vol. 7, pp. 93049–93061, 2019.

[5] A. Laib, A. Krama, A. Sahli, A. Kihal, and H. Abu-Rub, "Reconfigurable model predictive control for grid connected pv systems using thirteen-level packed e-cell inverter," *IEEE Access*, vol. 10, pp. 102210–102222, 2022.

[6] K. A. H. Daniel O. Johnson, "Issues of power quality in electrical systems," vol. 5, No. 4, pp. 148–154, 2016.

[7] H.Akagi, "Active harmonic filters," *proceeding of the IEEE*, vol. 93, December 2005.

[8] J. Sreedevi, N. Ashwin, and M. N. Raju, "A study on grid connected pv system," in *2016 National Power Systems Conference (NPSC)*, pp. 1–6, IEEE, 2016.

[9] H. KHAN, "Improving the performance of single phase power factor correction circuit using parallel boost converters," 2012.

[10] P. S.U.Prabha, "power quality issues , solutions and standards : a technology review," *applied science and engineering*, vol. 18, pp. 371–380, 2015.

[11] A. Y. M. U. H. Zia Hameed, Muhammad Rafay Khan Sial, "Harmonics in electrical power systems and how to remove them by using filters in etap," 2020.

[12] J. A. R.Waston and Neville, *power system harmonics second edition.* 2003.

[13] "Ieee recommended practice and requirements for harmonic control in electric power systems," *IEEE standards association*, 2014.

[14] B. R. T.Chandra Sekar, "A review and study of harmonic metigation techniques," *IEEE*, 2012.

[15] K. A.-H. B. Singh and A. Chandra, "A review of active filters for power quality improvement," *IEEE Transactions on Industrial Electronics*, vol. 46, october, 1999.

[16] T. Markvart and L. Castañer, *Practical handbook of photovoltaics: fundamentals and applications.* Elsevier, 2003.

[17] X. H. Nguyen and M. P. Nguyen, "Mathematical modeling of photovoltaic cell/module/arrays with tags in matlab/simulink," *Environmental Systems Research*, vol. 4, pp. 1–13, 2015.

[18] InTechOpen, "Modeling of photovoltaic module." https://www.intechopen.com/chapters/75972. (accessed: May 25, 2022).

[19] G. M. Masters, *Renewable and efficient electric power systems.* John Wiley & Sons, 2013.

[20] G. N. Tiwari and S. Dubey, *Fundamentals of photovoltaic modules and their applications*. Royal Society of Chemistry, 2009.

[21] Y. A. Amor, N. A. Amor, and A. KHELDOUN, *Design of Grid Connected Photovoltaic System*. LAP LAMBERT Academic Publishing, 2018.

[22] W. Zhang, P. Mao, and X. Chan, "A review of maximum power point tracking methods for photovoltaic system," in *2016 IEEE International Conference on Sustainable Energy Technologies (ICSET)*, pp. 230–234, IEEE, 2016.

[23] A. Mohapatra, B. Nayak, P. Das, and K. B. Mohanty, "A review on mppt techniques of pv system under partial shading condition," *Renewable and Sustainable Energy Reviews*, vol. 80, pp. 854–867, 2017.

[24] P. Asuri, "Chapter 2: Single phase pulse width modulated inverters," technical report, Tennessee Technological University, 2015. Accessed: 2025-06-14.

[25] F. Sebaaly, M. Sharifzadeh, H. Y. Kanaan, and K. Al-Haddad, "Multilevel switching-mode operation of finite-set model predictive control for grid-connected packed e-cell inverter," *IEEE Transactions on Industrial Electronics*, vol. 68, no. 8, pp. 6992–7001, 2020.

[26] M. H. Bollen and F. Hassan, *Integration of distributed generation in the power system*. John wiley & sons, 2011.

[27] M. Singh and S. Mahapatra, "Implementation of passive filters for harmonics reduction," *Int. J. Adv. Sci. Technol*, vol. 78, no. 1, pp. 1–12, 2015.

[28] H. Akagi, "Active harmonic filters," *Proceedings of the IEEE*, vol. 93, no. 12, pp. 2128–2141, 2005.

[29] A. Ghosh and G. Ledwich, *Power quality enhancement using custom power devices*. Springer science & business media, 2012.

[30] M. El-Habrouk, M. Darwish, and P. Mehta, "Active power filters: A review," *IEE Proceedings-Electric Power Applications*, vol. 147, no. 5, pp. 403–413, 2000.

[31] F. Sebaaly, M. Sharifzadeh, H. Y. Kanaan, and K. Al-Haddad, "Multi-level switching-mode operation of finite-set model predictive control for grid-connected packed e-cell inverter," *IEEE Transactions on Industrial Electronics*, vol. 68, no. 8, pp. 6992–7001, 2020.

[32] A. N. H. Akagi, Y. Kanazawa, "Generalized theory of the instantaneous reactive power in three-phase circuits," *IPEC'83 - Int. Power Electronics Conf*, 1983.

[33] J. M. João Afonso, Carlos Couto, "Active filters with control based on the p-q theory," *IEEE Industrial Electronics Society Newsletter*, vol. 47, september ,2000.

[34] M. A. Edson H. Watanabe, Hirofumi Akagi, "The p-q theory for active filter control: Some problems andsolutions," 2004.

[35] M. A. E. H. Watanabe, R. M. Stephan, "New concepts of instantaneous active and reactive powers in electrical systems with generic loads,," *IEEE Trans. Power Delivery*, vol. 8, April 1993.

[36] E. H. W. M. Aredes, "New control algorithms for series and shunt three-phase four-wire active power filters," *IEEE Trans. Power Delivery*, vol. 10, July 1995.

[37] H. Akagi, Y. Kanazawa, and A. Nabae, "Instantaneous reactive power compensators comprising switching devices without energy storage components," *IEEE Transactions on industry applications*, no. 3, pp. 625–630, 1984.

[38] V. Khadkikar, A. Chandra, and B. N. Singh, "Generalised single-phase pq theory for active power filtering: simulation and dsp-based experimental investigation," *IET Power Electronics*, vol. 2, no. 1, pp. 67–78, 2009.

[39] S. Khettab, A. Kheldoun, R. Bradai, A. Oubelaid, S. Kumar, and N. Khosravi, "Performance evaluation of puc7-based multifunction single-phase solar active filter in real outdoor environments: Experimental insights," *IET Renewable Power Generation*, vol. 18, no. 11, pp. 1740–1757, 2024.

[40] S. Khettab, A. Kheldoun, and R. Bradai, "A novel runge-kutta-based model predictive controller for puc7-based single-phase shunt active power filter," *Computers and Electrical Engineering*, vol. 123, p. 110051, 2025.

[41] T. Santos, J. Pinto, P. Neves, D. Gonçalves, and J. L. Afonso, "Comparison of three control theories for single-phase active power filters," in *2009 35th Annual Conference of IEEE Industrial Electronics*, pp. 3637–3642, IEEE, 2009.

[42] J. G. Oliveira Pinto, R. Macedo, V. Monteiro, L. Barros, T. Sousa, and J. L. Afonso, "Single-phase shunt active power filter based on a 5-level converter topology," *Energies*, vol. 11, no. 4, p. 1019, 2018.

[43] A. Plunkett, "A current-controlled pwm transistor inverter drive," in *IEEE/IAS Annual Meeting*, pp. 785–792, 1979.

[44] G. Ganesan, K. Mishra, A. Jayaprakash, and P. Sureshbabu, "Simulation study of hysteresis current controlled single-phase inverters for photovoltaic systems with reduced harmonics level," *International Journal of Applied Engineering Research*, vol. 13, pp. 4409–4414, 2018.

[45] A. Sahli, F. Krim, A. Laib, and B. Talbi, "Model predictive control for single phase active power filter using modified packed u-cell (mpuc5) converter," *Electric Power Systems Research*, vol. 180, p. 106139, 2020.

[46] H. Rezk and A. M. Eltamaly, "A comprehensive comparison of different mppt techniques for photovoltaic systems," *Solar energy*, vol. 112, pp. 1–11, 2015.